The Plant Cell, Vol. 24: 3219–3234, August 2012, www.plantcell.org

LARGE-SCALE BIOLOGY ARTICLE

Ontogeny of the Maize Shoot Apical Meristem[W][OA]

Elizabeth M. Takacs,[a] Jie Li,[b] Chuanlong Du,[b] Lalit Ponnala,[c] Diane Janick-Buckner,[d] Jianming Yu,[e] Gary J. Muehlbauer,[f] Patrick S. Schnable,[g] Marja C.P. Timmermans,[h] Qi Sun,[c] Dan Nettleton,[b] and Michael J. Scanlon[a,1]

[a] Department of Plant Biology, Cornell University, Ithaca, New York 14583
[b] Department of Statistics and Statistical Laboratory, Iowa State University, Ames, Iowa 50011
[c] Computational Biology Service Unit, Cornell University, Ithaca, New York 14853
[d] Division of Science, Truman State University, Kirksville, Missouri, 63501
[e] Department of Agronomy, Kansas State University, Manhattan, Kansas 66506
[f] Department of Agronomy and Plant Genetics, University of Minnesota, St. Paul, Minnesota 55108
[g] Department of Agronomy, Iowa State University, Ames, Iowa 50011
[h] Cold Spring Harbor Laboratory, Cold Spring Harbor, New York 11724

The maize (*Zea mays*) shoot apical meristem (SAM) arises early in embryogenesis and functions during stem cell maintenance and organogenesis to generate all the aboveground organs of the plant. Despite its integral role in maize shoot development, little is known about the molecular mechanisms of SAM initiation. Laser microdissection of apical domains from developing maize embryos and seedlings was combined with RNA sequencing for transcriptomic analyses of SAM ontogeny. Molecular markers of key events during maize embryogenesis are described, and comprehensive transcriptional data from six stages in maize shoot development are generated. Transcriptomic profiling before and after SAM initiation indicates that organogenesis precedes stem cell maintenance in maize; analyses of the first three lateral organs elaborated from maize embryos provides insight into their homology and to the identity of the single maize cotyledon. Compared with the newly initiated SAM, the mature SAM is enriched for transcripts that function in transcriptional regulation, hormonal signaling, and transport. Comparisons of shoot meristems initiating juvenile leaves, adult leaves, and husk leaves illustrate differences in phase-specific (juvenile versus adult) and meristem-specific (SAM versus lateral meristem) transcript accumulation during maize shoot development. This study provides insight into the molecular genetics of SAM initiation and function in maize.

INTRODUCTION

Plant shoots develop new leaves, stems, and buds throughout the life cycle via the maintenance of an organogenic population of stem cells within the stem cell niche or shoot apical meristem (SAM). These dual SAM functions of stem cell maintenance and organogenesis are ultimately responsible for the production of all aboveground plant tissues. Angiosperm SAMs display histological stratification into the clonally distinct tunica (outer) and corpus (inner) cell layers and are subdivided into the stem cells of the central zone and the organogenic peripheral zone. The maize (*Zea mays*) SAM forms during embryogenesis and persists until it transitions into an inflorescence meristem that ultimately forms the pollen-bearing tassel. Despite the vital importance of the SAM during plant shoot development, little is known about the molecular genetics of SAM ontogeny.

[1] Address correspondence to mjs298@cornell.edu.
The author responsible for distribution of materials integral to the findings presented in this article in accordance with the policy described in the Instructions for Authors (www.plantcell.org) is: Michael J. Scanlon (mjs298@cornell.edu).
[W] Online version contains Web-only data.
[OA] Open Access articles can be viewed online without a subscription.
www.plantcell.org/cgi/doi/10.1105/tpc.112.099614

Although maize embryos do not display stereotypical patterns of cell division, fate mapping confirms that cells occupying specific positions in the developing embryo correlate with predictable cell fates (Poethig et al., 1986). In addition, stage-specific morphological (Randolph, 1936; Abbe and Stein, 1954) and transcriptional landmarks (Nardmann and Werr, 2009) are described to identify key events in maize embryogenesis, including before SAM formation, during the transition to SAM initiation, and after the SAM is competent to form lateral organs. For example, transcript accumulation of the homeobox transcription factor *KNOTTED1* (*KN1*) is used as a marker for maize stem cell maintenance that is not detected in lateral organ primordia or anlagen (Smith et al., 1992; Jackson et al., 1994). The premeristematic proembryo contains no lateral organs and comprises a radially symmetrical embryo proper and a basal suspensor that do not accumulate *KN1* transcripts (Figures 1A and 1G; see Supplemental Table 1 online) (Smith et al., 1995). Two morphological events describe the transition-stage embryo: (1) formation of the SAM, marked by *KN1* expression, on the lateral face of the embryo; and (2) elaboration of the scutellum from the abgerminal face of the embryo (Figures 1B and 1H). A grass-specific lateral organ of controversial homology, the scutellum is specialized to absorb nutrients from the

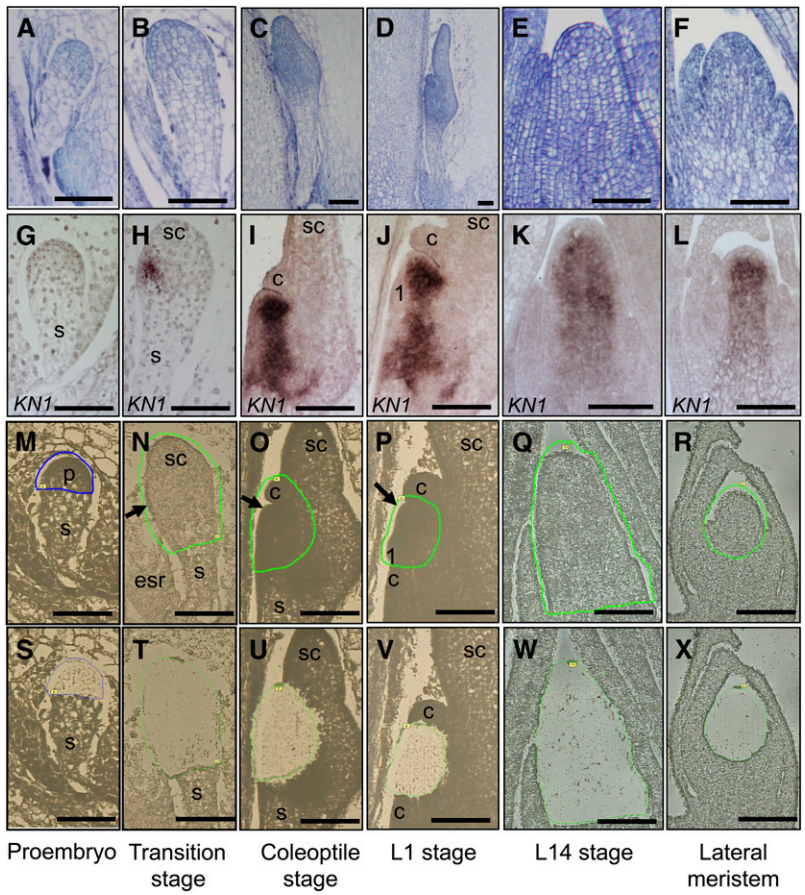

Figure 1. SAM Formation and Organ Initiation.

Toluidine blue O-stained embryos at key stages in embryo development (proembryo **[A]**, transition stage **[B]**, coleoptile stage **[C]**, and L1 stage **[D]**) and the SAM **(E)** and lateral meristem **(F)** from 14-d-old seedlings. In situ hybridization showing transcript accumulation of *KN1* during embryogenesis (**[G]** to **[J]**) and in the SAM **(K)** and lateral meristem **(L)** of a 14-d-old seedling. Before and after laser microdissection of maize embryos (**[M]** to **[P]** and **[S]** to **[V]**) and SAM (**[Q]** and **[W]**) and lateral meristem (**[R]** and **[X]**) from 14-d-old seedlings. The area selected for laser microdissection is outlined in blue or green. Arrows point to meristem. 1, leaf 1; c, coleoptile; esr, embryo-surrounding region; p, embryo proper; s, suspensor; sc, scutellum.
Bars = 100 μm.
(Figure 1E *courtesy of Addie Thompson*.)

endosperm during seedling germination. During the coleoptilar stage, a bikeeled leaf-like coleoptile initiates from the abgerminal side of the newly ramified meristem and ultimately forms a protective sheath surrounding the embryonic shoot (Figure 1C). At this stage, *KN1* transcripts are detectable throughout the dome-shaped SAM but are excluded from the meristem periphery, where the coleoptile emerges (Figure 1I).

Three distinct models have been proposed to debate the homology of the maize cotyledon (Weatherwax, 1920; Boyd, 1931; Kaplan, 1996). One model proposes that the coleoptile is the maize cotyledon, and the scutellum is a novel evolutionary innovation that arose in the grasses (Boyd, 1931). A second model suggests that the scutellum comprises the cotyledon, whereas the coleoptile is a foliar leaf (Weatherwax, 1920). Others have argued that the maize cotyledon is a bimodal structure in which the scutellum forms the distal tip and the coleoptile forms the sheathing base of the single cotyledon (Kaplan, 1996). Providing evidence for the bimodal cotyledon, maize displays distichous phyllotaxy (leaves emerge from opposite sides of the stem and in two ranks), and the scutellum and coleoptile both initiate from the abgerminal side of the embryo (Kaplan, 1996). Formation of the first foliar leaf from the germinal flank of the domed SAM (opposite the scutellum and the coleoptile) occurs during stage 1 (L1; Figure 1D), whereupon *KN1* transcripts accumulate in the embryonic shoot–root axis but not at sites of leaf initiation (Figure 1J). Once established, leaf initiation continues in a distichous phyllotactic pattern until the embryonic SAM has initiated up to five or six leaves, whereupon development is interrupted during seed quiescence. Upon germination, the SAM resumes its dual functions of stem cell maintenance and leaf initiation (Figures 1E and 1K). Similar to the SAM, lateral shoot meristems undergo vegetative growth, first initiating a bikeeled prophyll followed by foliar husk leaves before transitioning into an inflorescence meristem or undergoing senescence (Figures 1F and 1L) (Kiesselbach, 1949).

Previous studies have analyzed transcripts encoded in various hand-dissected and laser-microdissected shoot apices from 14-d-old seedlings using microarray analysis, as well as 454-based and Illumina-based RNA sequencing (RNA-seq) (Emrich et al., 2007; Ohtsu et al., 2007; Brooks et al., 2009; Jia et al., 2009; Nogueira et al., 2009). However, as yet, no transcriptomic analyses of maize SAM ontogeny during embryogenesis have been described. In this study, laser microdissection of specific domains during landmark developmental stages in embryogenesis is combined with RNA-seq technology to generate a transcriptional profile of the developing maize SAM and embryonic lateral organs. Five main questions are addressed in this article. First, what changes in transcript accumulation characterize the initiation of the embryonic SAM, and when are the dual meristematic functions of stem cell maintenance and organogenesis established? Second, what transcripts distinguish a newly formed embryonic meristem from a meristem that is mature and initiating foliar leaves? Third, what are the transcriptomic differences during initiation of the first three embryonic lateral organs—the scutellum, coleoptile, and first leaf? Fourth, what transcriptional profiles distinguish embryonic leaves from leaves made from the adult-staged SAM after seedling germination? Fifth, what transcriptomic differences distinguish the SAM from the lateral branch meristems that give rise to the ear inflorescence?

RESULTS AND DISCUSSION

Laser Microdissection and RNA-Seq of SAM Ontogeny

Laser microdissection enables the isolation of discrete domains within microscopic samples for use in transcriptomic analyses (Nelson et al., 2006; Scanlon et al., 2009). Six samples were microdissected from developing embryos and 14-d-old seedlings, including (1) the cells comprising the embryo proper of the proembryo (Figures 1M and 1S), (2) the organizing SAM and emerging scutellar hood of the transition-stage embryo (Figures 1N and 1T), (3) the SAM and the initiating coleoptile of the coleoptile-stage embryo (Figures 1O and 1U), (4) the SAM and leaf primordium of a stage 1 embryo (Figures 1P and 1V), (5) the SAM and plastochron 1 leaf of a 14-d-old seedling (L14; Figures 1Q and 1W), and (6) the lateral meristem and the newly initiated husk leaf from the 14-d-old seedling (Figures 1R and 1X). Two biological replicates were obtained per sample; replicates comprised cells from three to eight separate embryos or seedlings (see Supplemental Table 2 online). Total RNA isolated from the microdissected cells was subjected to two rounds of linear amplification to generate microgram quantities of RNA amenable to RNA-seq analyses (reviewed in Brooks et al., 2009). Amplified RNA was used to construct cDNA libraries, and Illumina-based RNA-seq generated a total of 130 million 44-bp sequence reads that were aligned to the maize genome (see Methods; Schnable et al., 2009). A summary of the total number of reads per biological replicate and their alignment to the maize gene space is presented in Supplemental Table 2 online. Read counts for each transcript were normalized to account for variation in library size across the 12 samples and are reported as reads mapped per million mapped sequences (RPM) (see Methods). Note that the RNA amplification step, which uses the polyA tail of the mRNA, excludes noncoding RNAs from the data set. Pairwise comparisons between each of the six samples and a comparison across the entire sample set were performed to identify differentially accumulated transcripts, taking into account false discovery rates (FDRs; see Methods). For all comparisons, an adjusted P value (q value $\leq$ 0.05) was used to identify upregulated transcripts.

Transcripts from a total of 20,610 genes are represented in the combined RNA-seq data sets (Figure 2A). There is little variation in the total number of genes represented among the six stages; the transition stage comprised the largest number of individual gene transcripts (16,454), whereas the coleoptile stage had the fewest (15,952). Oscillations in gene expression, wherein certain genes are used reiteratively during development, have been demonstrated to impose some limitations on the use of transcriptomic analyses of developmental ontogeny (Brady et al., 2007; Moreno-Risueno et al., 2010). Indeed, six-way comparisons of the transcriptional data sets identified 12,135 genes that are common to all samples (Figure 2A). Previous studies in maize and *Arabidopsis thaliana* guided the selection of candidate genes predicted to function during shoot development, which were surveyed for transcriptional patterns across the six samples. The 226 selected candidate genes were dispersed into seven developmental categories, including stem cell maintenance, lateral organ initiation, dorsiventral patterning, chromatin structure and remodeling, hormonal signaling, apical-basal patterning, and cell division and growth. A heat map was generated based on the relative transcript accumulation of each candidate gene during the six SAM developmental stages, revealing dynamic changes in transcriptional pattern before and after formation of the meristem, after the nascent meristem becomes functionally mature, during elaboration of three distinct lateral organ types (i.e., the scutellum, the coleoptile, and the leaf), and during initiation of juvenile, adult, and husk leaves (Figure 2B) (see Supplemental Data Set 1 online). These summary data confirm that the combined strategies of laser microdissection and RNA-seq can successfully detect transcriptional differences on a global scale.

Establishing a Meristem

To identify SAM-specific gene transcripts, transcript accumulation in the premeristematic proembryo was compared with all samples microdissected after SAM formation (i.e., the transition stage, the coleoptile stage, the L1 stage, the L14 stage, and lateral meristems). A total of 4145 gene transcripts were either upregulated or present/absent in comparisons of the proembryo with meristem-containing samples (see Methods; Figure 3A; see Supplemental Data Set 2 online). Of the 4145 gene transcripts represented, 284 are present in the proembryo and absent from samples containing a meristem, whereas 742 are unique to samples containing a meristem (Figure 3A). These 742 meristem-specific genes were distributed into MapMan functional categories, and more than one-half of the predicted gene products fell into three categories: transcriptional regulation (123 genes), genes that function in transport (103 genes), and genes of unknown function (271 genes) (Figure 3C; see Supplemental

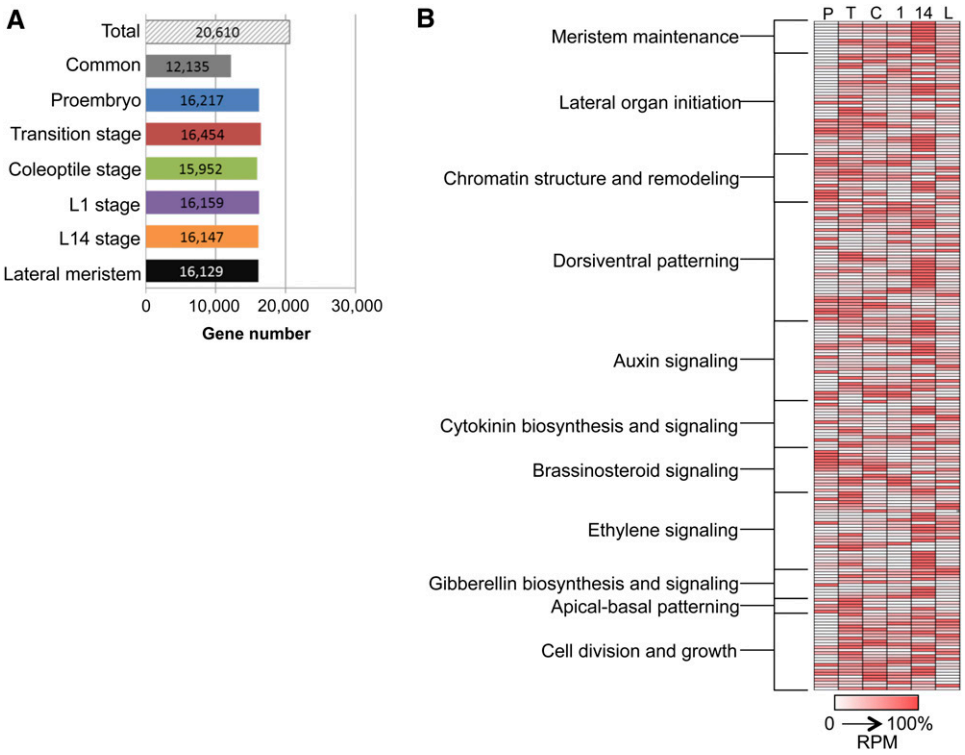

Figure 2. Genes Represented in Each of the Six RNA-Seq Data Sets.

(A) All genes represented in each of the six samples (RPM ≥ 1).

(**B**) Heat map based on the relative transcript accumulation of 226 candidate genes sorted according to implicated function. 1, L1 stage; 14, L14 stage; C, coleoptile stage; L, lateral meristem; P, proembryo; T, transition phase.

Data Set 3 online) (Thimm et al., 2004). Nineteen genes implicated in transcriptional regulation were exclusively detected in the premeristematic proembryo, whereas 123 were found only in samples containing a meristem (Figure 3B). These 123 meristematic genes that function in transcriptional regulation were sorted into gene families of known predicted function (Figure 3D; see Supplemental Data Set 4 online).

Transcription factors implicated in stem cell maintenance include six *CLASS I KNOTTED1-LIKE HOMEOBOX* (*KNOX*) genes and three *BEL-LIKE* (*BELL*) *HOMEOBOX* genes; CLASS I KNOX and BELL proteins form heterodimers that regulate stem cell identity (see Supplemental Data Set 3 online) (Reiser et al., 2000; Bellaoui et al., 2001; Müller et al., 2001; Smith et al., 2002; Mukherjee et al., 2009; reviewed in Hay and Tsiantis, 2010). At least two gene transcripts encoding WUSCHEL-RELATED HOMEODOMAIN (WOX) proteins (WOX2A and WOX9B) were upregulated in the proembryo. In *Arabidopsis*, *WOX2* and *WOX9* (also known as *STIMPY*) are also expressed before SAM initiation and specify the apical-basal axis of the embryo (Haecker et al., 2004; Wu et al., 2007; Breuninger et al., 2008). Previous reports in maize revealed that *WOX2A* transcripts accumulate in the apical cap of the proembryo before localizing to the germinal face of the transition-stage embryo (Nardmann et al., 2007). The accumulation of *WOX2A* and *WOX9B* transcripts in the premeristematic maize proembryo is consistent with a conserved function of these WOX putative paralogs in establishing apical-basal domains in the maize embryo before SAM initiation.

Transcripts encoding transcription factors that are known to function during organogenesis and that are not detected in the proembryo include members of the *YABBY* (six), *GROWTH-REGULATING FACTOR* (*GRF*, four), and *NO APICAL MERISTEM/CUP-SHAPED COTYLEDON* (four) gene families (the numbers in parentheses represent the number of transcripts in that gene family) as well as two additional *WOX* transcripts (Aida et al., 1999; Kim et al., 2003; Vroemen et al., 2003; Juarez et al., 2004; Zimmermann and Werr, 2005; Nardmann et al., 2007; Zhang et al., 2008; Sarojam et al., 2010; Santa-Catarina et al., 2012). Previous studies in *Arabidopsis* and maize demonstrated that *YABBY* genes are expressed in leaf and floral anlagen and in the marginal tips of leaf and floral primordia (Siegfried et al., 1999; Juarez et al., 2004). Consistent with these previous findings, transcript accumulation of *Zea mays YABBY14* (*ZYB14*), *Zea mays YABBY9* (*ZYB9*), and *Zea mays YABBY10* (*ZYB10*) was upregulated in samples containing a meristem as compared with the proembryo stage (Juarez et al., 2004). Furthermore, transcripts of the *Arabidopsis FILAMENTOUS FLOWER* (*FIL*; also known as *ABNORMAL FLORAL ORGAN* and *YABBY1*) and *YABBY3* (*YAB3*) accumulate in late globular-stage and heart-stage embryos, indicating that these putative YABBY paralogs also mark the initiating cotyledons (Siegfried et al.,

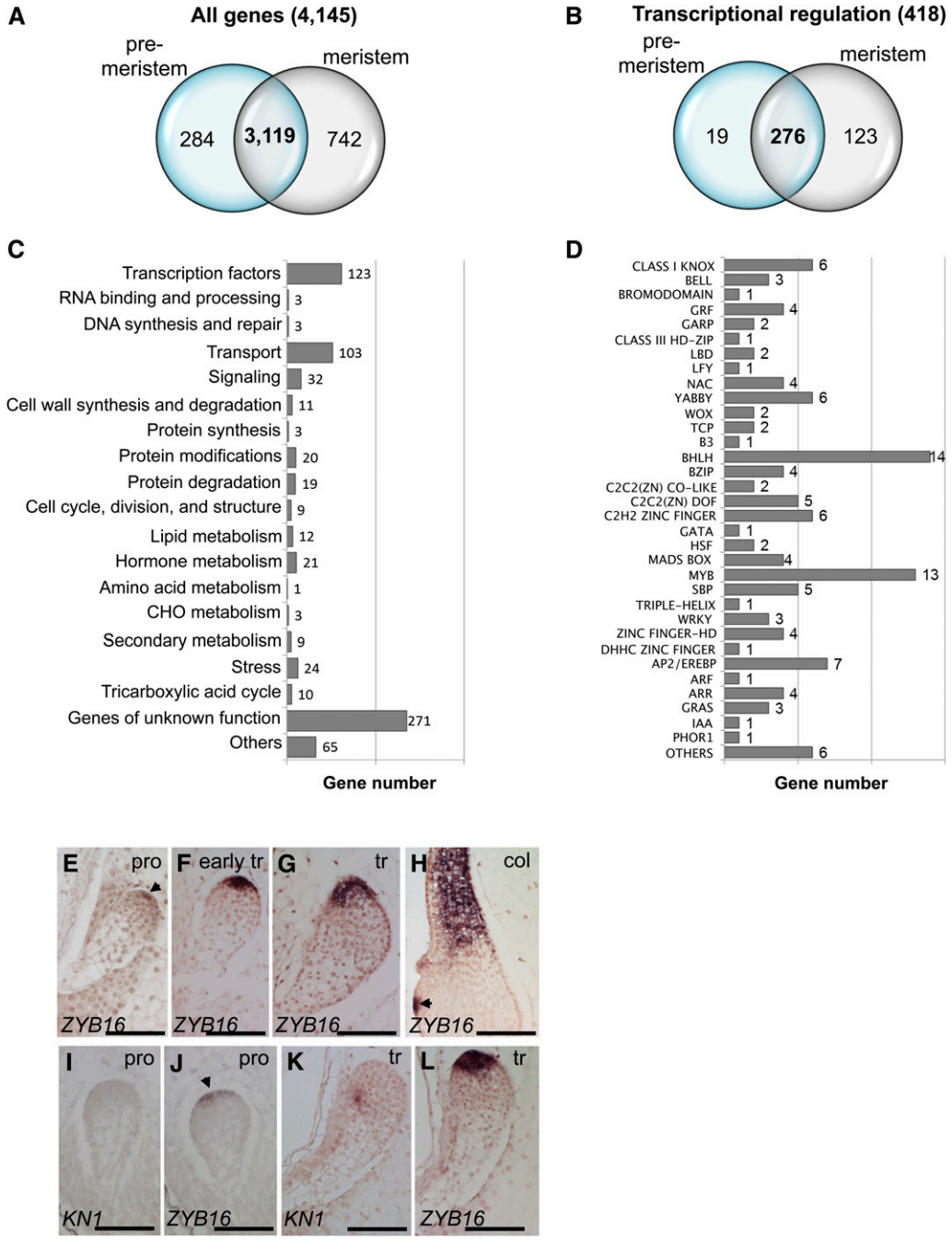

Figure 3. Establishing a Meristem.

(A) Venn diagram of all 4145 transcripts upregulated or present/absent in the premeristematic proembryo compared with the five samples with meristems. Transcripts in the overlapping region of the Venn diagram are present before and after the meristem forms, whereas transcripts in the nonoverlapping regions are present before but not after meristem formation or vice versa.

(B) The 418 out of the 4145 transcripts that are implicated in transcriptional regulation are presented in a Venn diagram.

(C) MapMan bin distribution of the 742 transcripts that are differentially accumulated after the meristem forms. CHO, carbohydrate.

(D) The 123 transcripts implicated in transcriptional regulation present after the meristem forms sorted into their respective gene product families. In situ hybridizations using *ZYB16* (**[E]** to **[H]**, **[J]**, and **[L]**) and *KN1* (**[I]** and **[K]**) probes. Arrowheads point to transcript accumulation. col, coleoptile stage; pro, proembryo; tr, transition phase.

Bars = 100 μm.

1999). Transcripts of another YABBY homolog, which we have designated *Zea mays YABBY16* (*ZYB16*), accumulate in the developing scutellum at the apex of the maize proembryo (Figure 3E). In addition, *ZYB16* transcripts are retained in the scutellar tip, in the initiating coleoptile, and in the anlagen of initiating leaves at later stages in embryogenesis (Figures 3F to 3H). These data suggest that the scutellum displays a pattern of *ZYB16* transcript equivalent to that of other lateral organs in the maize shoot, which is consistent with models ascribing leaf homology to the scutellum (Kaplan, 1996). Evidence from additional molecular markers, described below, lends further evidence to the hypothesis that the scutellum is a leaf-like lateral organ.

Moreover, in situ hybridizations performed using *KN1* and *ZYB16* probes on consecutive embryo sections of both proembryo (Figures 3I and 3J) and transition-stage samples (Figures 3K and 3L) confirm that the onset of *ZYB16* transcript accumulation precedes that of *KN1*. By contrast, control hybridizations reveal that both *KN1* and *ZYB14* transcripts first accumulate during the transition stage (see Supplemental Figures 1A to 1D online). Taken together, these data suggest that the dual functions of the maize SAM are not simultaneously activated during SAM ontogeny; lateral organ initiation, as indicated by accumulation of *ZYB16* transcripts, precedes stem cell maintenance in the maize SAM. These data extend and support the conclusions from previous analyses demonstrating that a maize mutant defective in meristem maintenance is capable of forming a scutellum and coleoptile, plus a few small leaves (Vollbrecht et al., 2000).

Morphological and Molecular Maturation of the Maize SAM

Significant morphological differences are recognized in a newly formed transition-stage shoot meristem and a mature, L14-stage SAM that has initiated multiple foliar leaves. At the transition stage, the meristem is flattened and composed of ~150 cells organized in longitudinal files at least two cell layers deep, which correlates with the transcript accumulation of the stem cell marker *KN1* in these embryos (Figures 1B and 1H) (Poethig et al., 1986; Smith et al., 1992; Jackson et al., 1994). Lateral organs are not initiated from the early transition-stage SAM; the scutellum forms during the proembryo stage (described previously), whereas the coleoptile does not initiate until the late transition/coleoptilar stage (Abbe and Stein, 1954). By contrast, the L14-stage SAM attains a postlike architecture comprising multiple cell layers organized into distinct functional zones and is actively initiating leaves (Figures 1E and 1K). To investigate the transcriptional changes that correlate with these morphological differences during SAM maturation, the transcriptome of the L14-stage SAM was compared with that of the newly formed transition-stage SAM. This comparison identified 1706 transcripts that were upregulated or present/absent during these developmental stages (Figure 4A; see Supplemental Data Set 5 online). Transcripts that fell into metabolic and regulatory MapMan functional categories are displayed in Supplemental Figures 2 and 3 online (see Supplemental Data Sets 6 and 7 online). A Fisher's exact test revealed that transcripts implicated to function in protein and mitochondrial electron transport/ATP synthesis are enriched in newly initiated SAMs, whereas in the L14 stage, SAM transcripts that function in hormone metabolism, transport, and transcriptional regulation are upregulated (see Methods; Figure 4B) (Thimm et al., 2004).

Enrichment of protein synthesis in transition-stage SAMs is consistent with previous findings that enhanced ribosome function is required to establish a shoot meristem (Weijers et al., 2001; Tzafrir et al., 2004; reviewed in Byrne, 2009). Transcripts encoding the maize RIBOSOMAL PROTEIN S5A and S5B (RPS5A, also known as *Arabidopsis* MINUTE-LIKE1 [AML1]; RPS5B) are both upregulated in transition-stage embryos compared with the L14-stage SAMs. Development of *aml1* mutant embryos is arrested at the globular stage in *Arabidopsis* before the meristem is established (Weijers et al., 2001). In addition, as compared with the L14-stage SAM, the transition-stage SAM contains more upregulated gene transcripts that are implicated in protein targeting (14:5), amino acid synthesis (19:9), and DNA synthesis and repair (24:11). These data suggest that an increase in ATP production and in DNA and protein metabolic activity immediately precedes the proliferative growth displayed during later stages of SAM ontogeny.

The dual functions of stem cell maintenance and lateral organ initiation occur concomitantly in mature L14-stage SAMs, as is reflected in the predicted functions of 109 transcripts implicated in transcriptional regulation that are upregulated at this stage. Among these are four transcripts encoding known stem cell regulators, including three *CLASS I KNOX* genes and a GATA domain protein homologous to HANABA TARANU in *Arabidopsis* (Figures 4C and 4D; see Supplemental Data Set 8 online) (Reiser et al., 2000; Zhao et al., 2004; Mukherjee et al., 2009; reviewed in Hay and Tsiantis, 2010). Upregulated transcripts encoding proteins that function in organogenesis and cell proliferation of lateral organs include *WUSHEL-RELATED HOMEOBOX3A* (*WOX3A*), the *YABBY* gene *DROOPING LEAF2* (*DL2*), the lateral organ boundary gene *INDETERMINATE GAMETOPHYTE1* (*IG1*), and two *GRF-LIKE* transcripts (Kim et al., 2003; Nardmann et al., 2004; Yamaguchi et al., 2004; Evans, 2007; Nardmann et al., 2007; Zhang et al., 2007; Zhang et al., 2008). In addition to three *AUXIN RESPONSE FACTOR* (*ARF*) class transcription factors, several transcripts that encode hormone biosynthetic proteins are also upregulated in stage 14 SAMs, including seven gibberellin metabolic transcripts implicated in lateral organ growth and development. Transcripts involved in ethylene and jasmonate signaling and regulation also accumulate differentially in mature, stage 14 SAMs (see Supplemental Figure 3 and Supplemental Data Set 7 online). These data suggest that, compared with the transition stage, the stage 14 meristem contains a wider diversity of transcripts implicated in both lateral organ initiation and stem cell maintenance.

Elaboration of the First Three Lateral Organs

Three different types of lateral organs are elaborated in maize embryos: the scutellum, the coleoptile, and five to six foliar leaves. A three-way comparison was made between the transition stage, the coleoptile stage, and the L1-staged shoot apex to determine the transcriptional differences correlated with the development of these morphologically distinct organs. A total of

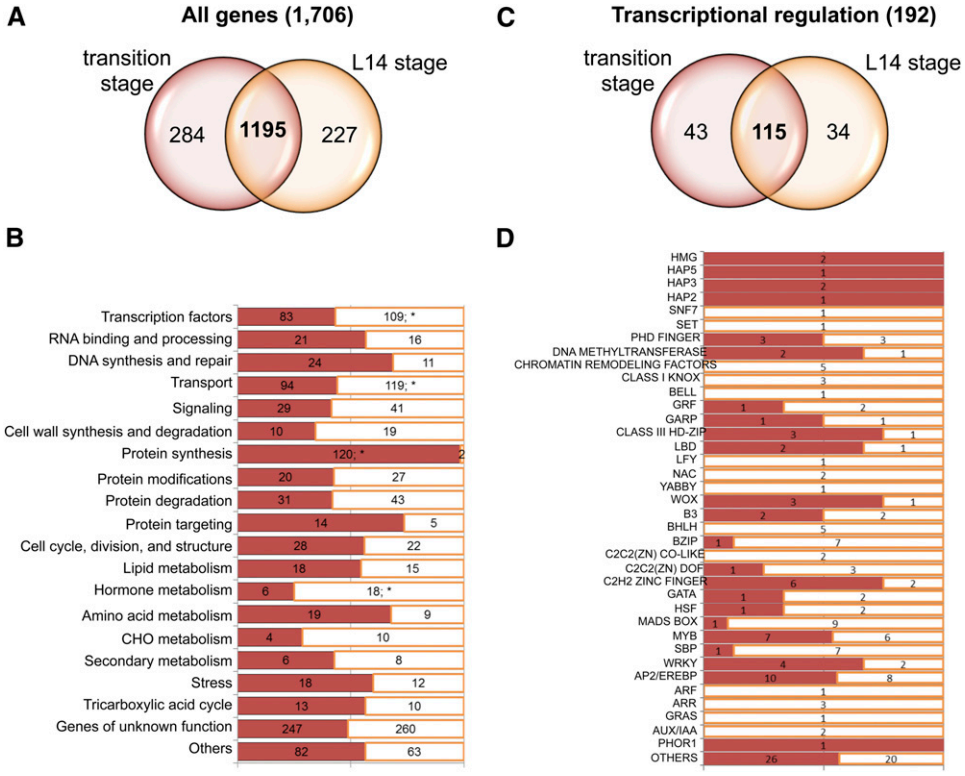

Figure 4. Transcriptomic Comparisons of a Newly Formed Meristem to a Mature Meristem.

(A) Venn diagram of the 1706 transcripts upregulated or present/absent when comparing the transition stage to the L14 stage. Transcripts in the overlapping region of the Venn diagram are present in both newly formed and mature meristems, whereas transcripts in the nonoverlapping regions are present before but not after meristem maturation or vice versa.

(B) The 1706 upregulated transcripts sorted into modified MapMan categories. Total number of transcripts in each functional category is displayed in the bars. Darker bars in **(B)** and **(D)** designate the transition stage, lighter bars indicate the L14 stage. Asterisk after transcript number indicates enrichment of that functional category using Fisher's exact test ($P \leq 0.01$; FDR, 6%). CHO, carbohydrate.

(C) The 192 out of 1706 transcripts upregulated or present/absent that are implicated in transcriptional regulation in a newly formed meristem and a mature meristem.

(D) The 192 transcripts are distributed into their respective gene product family.

532 transcripts were upregulated in the three-way comparison. Of these upregulated transcripts, 517 were sorted into three main clusters based on relative transcript abundance during the three embryonic stages. These include transcripts upregulated in the transition stage versus both the coleoptile and L1 stages (Figure 5A, cluster 1), transcripts upregulated in the transition stage versus the L1 stage (Figure 5A, cluster 2), and transcripts upregulated in the L1 stage versus the transition stage (Figure 5A, cluster 3) (see Supplemental Figure 4 and Supplemental Data Set 9 online). The 517 genes from the respective clusters were distributed into 25 MapMan annotated functional categories and were displayed in metabolic and regulatory pathways (Figure 5A, see Supplemental Figures 5 and 6 and Supplemental Data Sets 10 and 11 online) (Thimm et al., 2004). A total of 63 transcripts implicated in transcriptional regulation were present in the three main clusters, many of which have specific functions in embryo development, including but not limited to apical-basal patterning and cotyledon development (Figure 5B; see Supplemental Data Set 12 online).

Several transcripts encoding transcription factors implicated in apical-basal patterning of the embryo were upregulated during the transition stage, including *WOX2A*, *WOX5B*, and *NUTCRACKER* (*NUC*; Haecker et al., 2004; Levesque et al., 2006; Nardmann et al., 2007). Whereas WOX2 functions in the apical embryo domain, *WOX5* and *NUC* homologs accumulate in the basal regions of developing embryos, where they eventually specify distinct root domains (Haecker et al., 2004; Levesque et al., 2006; Nardmann et al., 2007). These root-specific transcription factors were probably detected in our transition-stage samples because these microdissected domains included both the apical and basal regions of the embryo (Figures 1N and 1T), whereas only shoot domains were isolated from later stages. Upregulated during development of both the scutellum and the coleoptile, the *HEME ACTIVATOR PROTEIN3* (*HAP3*) class transcription factor *Zea mays LEAFY COTYLDEON1* (*LEC1*) functions during lipid metabolism in maize, whereas homologs in *Arabidopsis* also specify cotyledon development (Mu et al., 2008; Shen et al., 2010). Fatty acid biosynthesis is especially

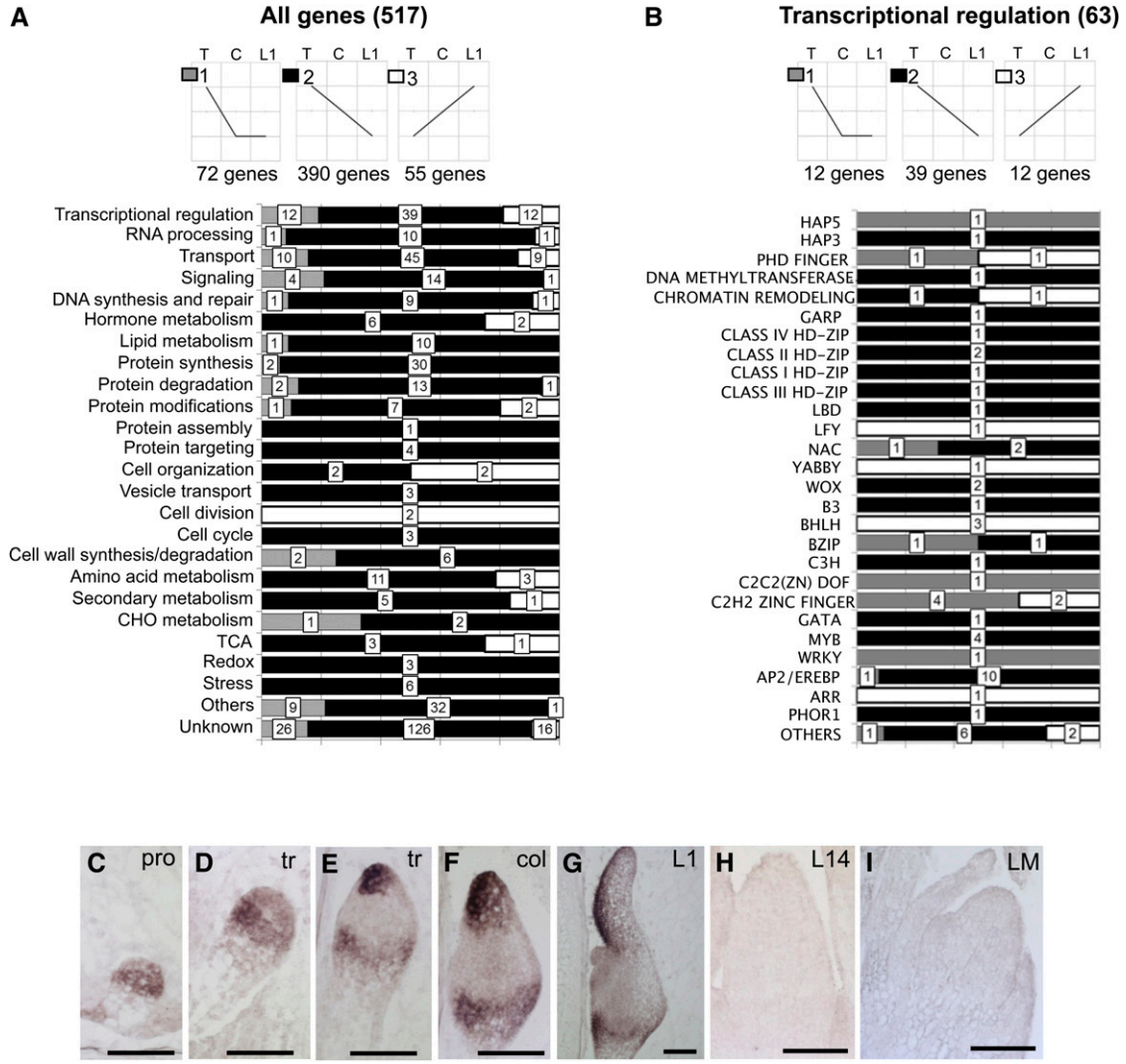

Figure 5. Elaboration of the Scutellum, the Coleoptile, and the First Foliar Leaf.

(A) Three main clusters that comprise 517 of 532 genes upregulated in the three-way comparison of the transition stage (T), coleoptile stage (C), and L1 stage (L1) embryos. Distribution of genes into functional categories according to MapMan. CHO, carbohydrate; TCA, tricarboxylic acid.

(B) The 63 genes that are implicated in transcriptional regulation from the three main clusters distributed into gene families. The transition stage is shaded gray, the coleoptile stage is shaded black, and the L1 stage is shaded white. In situ hybridizations illustrate the accumulation of *LEC1* transcripts during embryogenesis (**[C]** to **[G]**) and in 14-d-old seedlings (**[H]** and **[I]**). col, coleoptile stage; L1, leaf 1 stage; L14; 14-d-old seedling SAM; LM, lateral meristem; pro, proembryo; tr, transition phase.

Bars = 100 μm.

proliferative during embryogenesis, when oil bodies are stored as energy reserves that will subsequently be used during germination. Zm-*LEC1* is expressed throughout the apical cap in the proembryo and early transition stage (Figures 5C and 5D) (Zhang et al., 2002) but is restricted to the scutellar tip and base during the late transition stage (Figure 5E) before eventually localizing to the emerging coleoptile (Figure 5F). At the L1 stage, *LEC1* transcripts accumulate at the germinal side of the scutellar hood and at the boundary between the apical embryo and the basal suspensor (Figure 5G). As in *Arabidopsis*, no Zm-*LEC1* transcripts are detected in foliar leaves (Figures 5H and 5L) (Lotan et al., 1998; Suzuki et al., 2008; Shen et al., 2010). Accumulation of Zm-*LEC1* in both the scutellum and coleoptile, but not in maize embryonic foliar leaves, is likewise consistent with models in which the scutellum and the coleoptile comprise the apical and basal zones of the single maize cotyledon. Interestingly, only four transcripts are exclusively upregulated in the coleoptile stage versus the transition and/or L1 stages. One such transcript encodes the maize BASIC HELIX-LOOP-HELIX transcription factor PHYTOCHROME-INTERACTING FACTOR3-LIKE5 (PIL5); the PIL5 homolog in *Arabidopsis* functions to inhibit seed germination (cluster 5; see Supplemental Figure 4

online) (Oh et al., 2007). The relatively few transcripts exclusively upregulated during the coleoptile stage may indicate that the coleoptile transcriptome is inherently similar to that of both the scutellum and the foliar leaf. These data are consistent with models ascribing the dual identity of the coleoptile as a component of the cotyledon that also functions as a photosynthetic leaf-like organ.

Several gene transcripts upregulated at the L1 stage versus the transition stage are believed to have specific functions in foliar leaves, such as transcripts predicted to encode transcription factors regulating leaf size and leaf cell proliferation (i.e., *SPATULA*, *AINTEGUMENTA*, and *ENHANCED DOWNY MILDEW2*) (Mizukami and Fischer, 2000; Ichihashi et al., 2010; Tsuchiya and Eulgem, 2010). Additional examples include the YABBY-like transcription factor, which is implicated in leaf midrib formation (*DROOPING LEAF1* [*DL1*]), and homologs of the microRNA biogenesis gene (*SERRATE*; Clarke et al., 1999; Yamaguchi et al., 2004; Laubinger et al., 2008). Interestingly, *DL* transcripts accumulate in young leaf primordia but not in the coleoptile or scutellum of rice (*Oryza sativa*) embryos (Yamaguchi et al., 2004), which further indicates that the grass coleoptile attains some, but not all, foliar-leaf attributes.

Among the differentially accumulated transcripts identified in embryonic lateral organs are several that exhibit tissue/organ-specific expression and are useful markers of embryo development, including (1) the scutellum-specific *TAPETUM DETERMINANT1-LIKE* (*TDL1*), (2) the vasculature-specific *RAN BINDING PROTEIN2* (*RANBP2*), (3) the coleorhiza-specific *POLLEN OLE E I-LIKE* (*OLE*), and (4) two epidermis-specific maize *LIPID TRANSFER PROTEINS* (*LTP*1* and *LTP*2*). *TDL1* transcripts are first detected in the tip of the developing scutellar hood at the transition stage (Figure 6B) and in the outer cell layer of the scutellum in the coleoptile-stage and L1-stage embryos (Figure 6C). No *TDL1* transcripts accumulate in the proembryo or in the 14-d-old seedling SAM and lateral meristem (Figures 6A, 6D, and 6E). *RANBP2* transcripts accumulate in the developing vasculature of all lateral organs elaborated in the embryo and in 14-d-old seedlings (Figures 6F to 6J). *OLE* transcripts accumulate in the basal region of transition-stage embryos, opposite that of the apical expression described for the scutellum marker *ZYB16* (Figures 3F, 6K, and 6l). As development proceeds, *OLE* transcripts are restricted to the basal region of the embryo, which eventually defines the coleorhiza, a sheathing structure that surrounds the maize primary root (Figures 6M to 6O). The two protodermal markers, *LTP*1* and *LTP*2*, are expressed in the apical regions of the proembryo and early transition-stage embryo (Figures 6P and 6Q; see Supplemental Figures 7A and 7B online), whereupon these *LTP* transcripts accumulate in the emerging scutellum of the late transition-stage embryo (Figure 6R). Subsequently, *LTP*1* and *LTP*2* localize to the epidermal cell layer of embryonic lateral organs (Figures 6S and 6T; see Supplemental Figures 7C and 7D online).

Other useful developmental markers identified in our RNA-seq analyses include the homolog of an *Arabidopsis LIGHT-DEPENDENT SHORT HYPOCOTYLS1* and *ORYZA LONG STERILE LEMMA1* (*ALOG*) transcript *ALOG*1*, which is implicated during specification of organ boundaries, and two gene transcripts

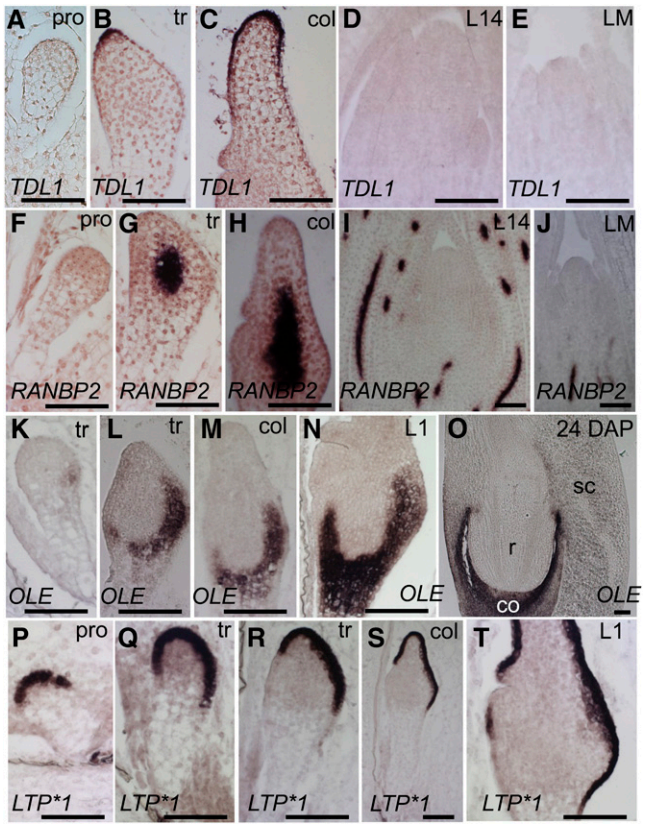

Figure 6. Differentially Accumulated Transcripts during the Elaboration of Embryonic Organs.

In situ hybridizations illustrate transcript accumulation of *TDL1* (**[A]** to **[E]**), *RANBP2* (**[F]** to **[J]**), *OLE* (**[K]** to **[O]**), and *LTP*1* (**[P]** to **[T]**). 24 DAP, embryo harvested 24 d after pollination; col, coleoptile stage; L1, leaf 1 stage; L14; 14-d-old seedling SAM; LM, lateral meristem; pro, proembryo; tr, transition phase.
Bars = 100 μm.

of unknown predicted function, designated as *UNKNOWN*1* (*UNK*1*) and *UNKNOWN*2* (*UNK*2*). In maize embryos, *ALOG*1* transcripts demarcate the boundary between all lateral organs and the developing SAM (Figures 7A to 7E). *UNK*1* transcripts first accumulate in a few cells at the site of organ initiation and then become localized to the adaxial side of the emerging lateral organ (Figures 7F to 7J). By contrast, *UNK*2* transcripts are detected in the growing edges of the sheath-like coleoptile (Figures 7K to 7O) and in the margins of all subsequent embryonic lateral organs. The similar accumulation patterns of these three transcripts during elaboration of the scutellum, coleoptile, and first foliar leaf further supports the model ascribing leaf homology to the scutellum and the coleoptile.

Comparative Transcriptomic Analyses of Juvenile, Adult, and Husk Foliar Leaves

Juvenile and adult foliar leaves of maize exhibit significant morphological differences. Juvenile leaves are short and narrow and accumulate epicuticular waxes but no epidermal hairs, and

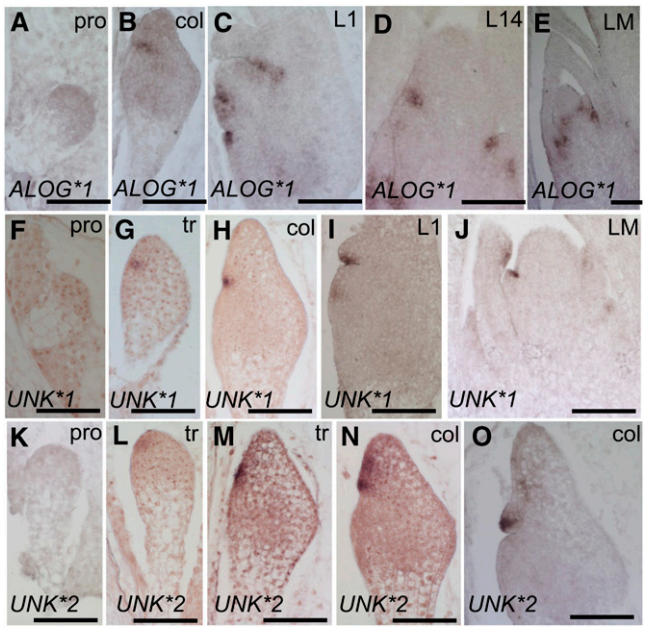

Figure 7. Developmental Markers Identified in RNA-Seq Analyses.

In situ hybridizations illustrate transcript accumulation of *ALOG*1* (**[A]** to **[E]**), *UNK*1* (**[F]** to **[J]**), and *UNK*2* (**[K]** to **[O]**). col, coleoptile stage; L1, leaf 1 stage; L14; 14-d-old seedling SAM; LM, lateral meristem; pro, proembryo; tr, transition phase.
Bars = 100 μm.

lateral meristems of juvenile nodes form long vegetative shoots tipped by a male inflorescence (tassel) (Poethig, 1988; Poethig, 1990; Moose and Sisco, 1994). By contrast, adult leaves are long and broad and have epidermal hairs but accumulate little epicuticular waxes, and adult lateral meristems form short branches that initiate husk leaves and form a female inflorescence (ear) (Poethig, 1988; Poethig, 1990; Moose and Sisco, 1994). Furthermore, leaves initiated from both the SAM and juvenile lateral meristems differ in many ways from husk leaves formed from adult-staged lateral meristems. Compared with foliar leaves, husk leaves have a lower vein density (Langdale et al., 1988), accumulate ribulose-1,5-bis-phosphate carboxylase/oxygenase in mesophyll as well as bundle sheath cells (Pengelly et al., 2011), and make a greater contribution to grain filling (Fujita et al., 1994; Sawada et al., 1995).

A complex interactive network of phase-specific transcription factors and regulatory small RNAs regulate vegetative and reproductive phase change in plants (Moose and Sisco, 1996; Lauter et al., 2005; Chuck et al., 2007; Hultquist and Dorweiler, 2008). To examine the transcriptional differences among juvenile-stage SAMs, adult-stage SAMs, and lateral shoot meristems from adult nodes on a genomic scale, the SAM and youngest leaf primordium were microdissected from L1-stage embryos and L14-stage seedlings, and lateral meristems were isolated from L14-stage seedlings. RNA-seq analyses and pairwise comparisons of these three microdissected samples identified a total of 5103 upregulated transcripts. A total of 12 major patterns (clusters) of transcript accumulation were identified in the three-way comparisons (Figure 8A). Cluster six is the largest and comprises 1121 transcripts that were upregulated at the L14 stage compared with the L1 stage. Other large clusters include (1) cluster 4 (886 transcripts), which comprises transcripts upregulated at the L14 stage compared with both the L1 stage and lateral meristem; (2) cluster 9 (596 transcripts), comprising transcripts upregulated in the lateral meristem compared with the L1 stage; and (3) cluster 2 (536 transcripts), which comprises transcripts upregulated in the L1 stage as compared with the L14 stage. A Fisher's exact test was performed to identify enriched functional groups within the 12 gene clusters (Figure 8B; see Supplemental Data Set 13 online). Functions enriched during the initiation of a juvenile leaf include RNA processing and binding (cluster 2); DNA synthesis, repair, and chromatin remodeling (cluster 3); protein synthesis and targeting (clusters 1 and 2); and the tricarboxylic acid cycle (cluster 1). The only category exclusively enriched in the lateral meristem is unknown function (cluster 9). Consistent with differences in cell wall composition between juvenile and adult foliar leaves, transcripts implicated in cell wall synthesis and degradation are enriched in both the L14-stage SAM and lateral meristems (cluster 12) (Abedon et al., 2006).

Transcription factors implicated in vegetative phase change were differentially expressed between juvenile and adult leaves. As previously described, eight *SQUAMOSA-PROMOTER BINDING PROTEIN-LIKE* (*SPL*) transcripts targeted by the juvenile-stage regulatory RNA miR156 were upregulated in the L14 stage and lateral meristems (see Supplemental Data Set 14 online) (Chuck et al., 2007; Hultquist and Dorweiler, 2008; Strable et al., 2008). In addition, *GLOSSY15* (*GL15*), an AP2-like transcription factor that promotes the adult leaf identity, is upregulated in 14-d-old seedlings (Evans et al., 1994; Moose and Sisco, 1996; Lauter et al., 2005). Transcriptional profiles of husk leaves are more similar to L14-stage than L1-stage leaves, as illustrated by the 417 gene transcripts that were upregulated in both the L14-stage SAM and the lateral meristem versus the L1-stage SAM and are displayed in metabolic and regulatory pathways (cluster 12) (see Supplemental Figures 8 and 9 and Supplemental Data Sets 15 and 16 online). This is consistent with previous studies showing that, once initiated, vegetative phase change is comprehensive and affects all subsequently elaborated organs of the maize shoot (Poethig, 1990).

Two transcripts upregulated during husk leaf initiation (*ALOG*2* and *LTP*3*) were analyzed by in situ hybridization. *ALOG*2* transcripts accumulate in the lateral organ boundaries of all three samples, suggesting a conserved function in defining foliar and husk leaves (Figures 8C to 8E). However, *LTP*3* transcripts accumulate in the outer cell layer of young leaf primordia and in the tunica of the lateral meristems but are excluded from the L1-stage and L14-stage SAMs (Figure 8B). Although the lateral meristem and the L14-stage SAM are both initiating vegetative leaves, a total of 1505 transcripts were upregulated (clusters 4, 5, 7, 8, 10, and 11), which reflects distinct developmental genetic mechanisms within these shoot meristems. The transcripts that are found in metabolic or regulatory pathways are displayed in Supplemental Figures 10 and 11 and Supplemental Data Sets 17 and 18 online.

In summary, the SAM transcriptome undergoes dynamic changes throughout the course of vegetative plant development.

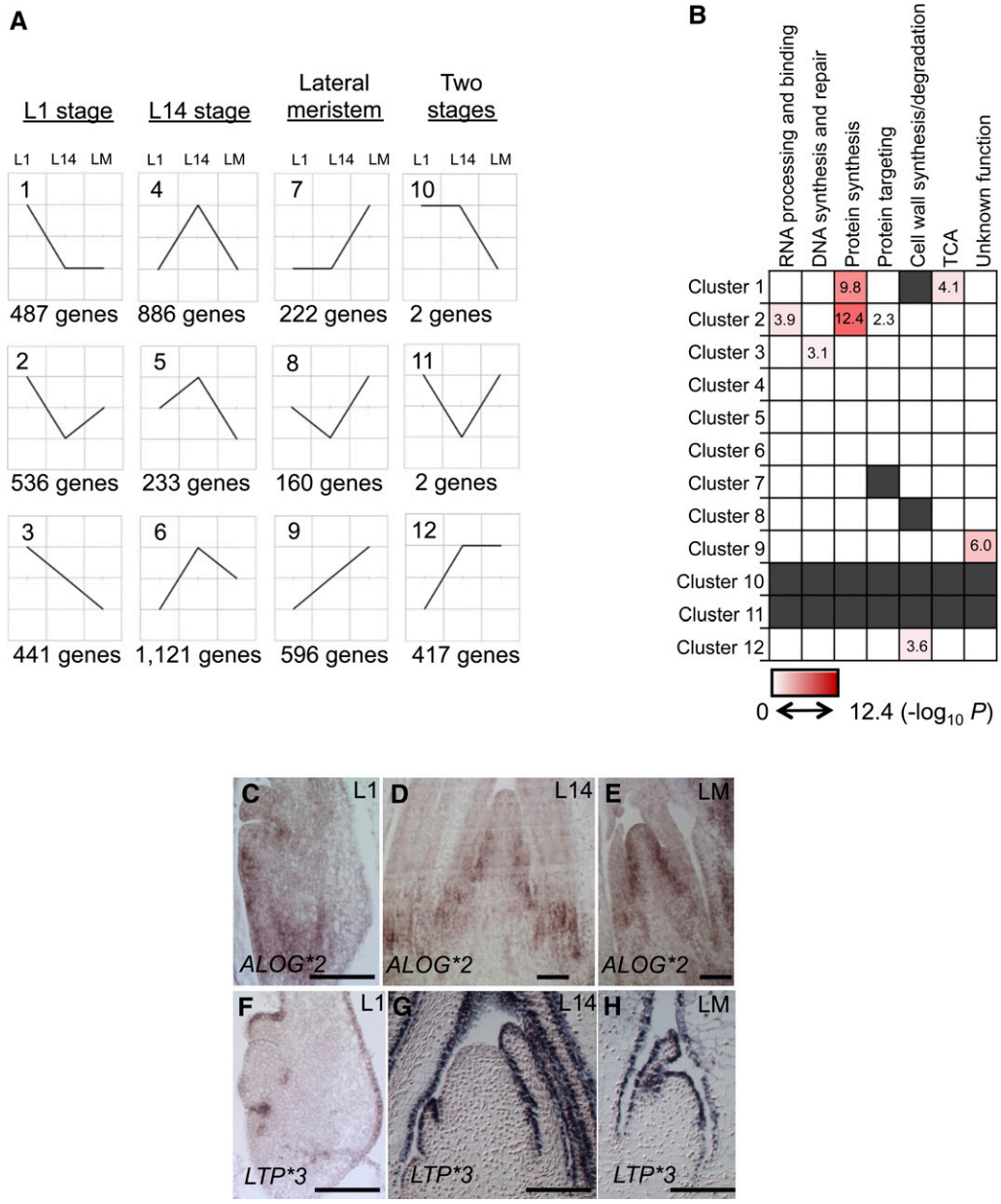

Figure 8. Initiation of Juvenile, Adult, and Husk Leaves.

(A) A total of 12 clusters were generated based on the transcript accumulation of the 5103 upregulated genes when making the three-way comparison of the L1 stage, L14 stage, and lateral meristem.

(B) Functional category enrichment of the 12 clusters. The $-\log_{10}$P value and FDR 5% are included for significant enrichment. White indicates nonsignificant enrichment, whereas red indicates significant enrichment. Gray indicates that no genes are present in the category for that cluster. In situ hybridizations using the following probes: *ALOG*2* (**[C]** to **[E]**), *LTP*3* (**[F]** to **[H]**). L1, leaf 1; L14, leaf 14; LM, lateral meristem; TCA, tricarboxylic acid. Bars = 100 μm.

Analysis of embryonic transcript accumulation before meristem formation identified *ZYB16*, a gene implicated in lateral organ initiation. Expression of *ZYB16* before *KN1* suggests that SAM function during organogenesis precedes that of stem cell maintenance. Transcriptomic analysis of a newly formed SAM indicates that, at this early developmental stage, the embryonic shoot is still establishing apical/basal domains and accumulating storage products to be used during the proliferative organogenesis and growth that defines later stages of maize embryo development. By contrast, the mature maize SAM is enriched for transcripts that function in transcriptional regulation, hormone signaling and metabolism, and transport. Transcriptomic analyses

of the three distinct types of lateral organs elaborated during embryogenesis provide support for models ascribing the maize cotyledon as a leaf-like, bimodal structure that comprises both the scutellum and the coleoptile. Finally, three-way comparisons between the initiation of juvenile, adult, and husk leaves reveal phase-specific and meristem-specific differential transcript accumulation. Novel molecular markers are identified that specify the cotyledon, the scutellum, the vasculature, the coleorhiza, initiating lateral organs, lateral organ boundaries, (Sen et al., 2009) and the protoderm or epidermis. Finally, all these transcriptomic data are publicly available at the Maize Genetics and Genomics Database (MaizeGDB; www.maizegdb.org) (Sen et al., 2009).

METHODS

Plant Growth Conditions and Sample Preparation

To prepare SAM and lateral meristems from 14-d-old seedlings, plants from a B73 background were grown in a growth chamber with a cycle of 16 h of light at 25°C and 8 h of dark at 22°C. We note that it is not possible to synchronize the developmental timing of maize embryogenesis such that the sample pools contained individual embryos from various time points within a single plastochron, or within a single embryonic stage for samples collected before stage 1. The effects of this unavoidable variability in developmental staging are lessened by pooling three to eight individual embryos per sample. Seedlings harvested 14 d after planting were dissected to remove roots and excess shoot structures as described previously (Scanlon et al., 2009). To prepare embryo samples, plants from a B73 inbred background grown to maturity were self-pollinated. The tips of whole kernels harvested from 5 to 13 d after pollination were excised and discarded to allow the fixative to infiltrate the remainder of the kernel that contains the embryo.

Tissue Fixation, Embedding, Sectioning, and Laser Microdissection

The 14-d-old SAM and lateral meristem samples and the kernel samples containing the developing embryos were fixed overnight at 4°C in Farmer's Fixative (3:1 ethanol:acetic acid) and dehydrated. After fixation, samples were prepared as described previously (Scanlon et al., 2009). Briefly, the samples were run through an ethanol/xylene series followed by a xylene/paraplast series before being embedded in paraplast. Embedded samples were sectioned using a rotary microtome (RM 2235; Leica Microsystems). The 10-μm-thick sections from the 14-d-old seedling and kernel samples were mounted on VWR VistaVision HistoBond Adhesive Slides (VWR International) with diethylpyrocarbonate-treated deionized water. The slides with the sectioned samples were dried overnight at 40°C and then stored in a sealed vacuum chamber until laser microdissection was performed. Laser microdissection was performed using a PALM Laser Microbeam (P.A.L.M. Microlaser Technologies) using version 3.0.0.9 software.

RNA Isolation and Amplification

Total RNA was isolated from the collected cells using the Arcturus PicoPure RNA Isolation Kit (Applied Biosystems). DNaseI treatment was performed during the RNA isolation using Qiagen DNaseI. RNA amplification was performed using the TargetAmp 2-Round Aminoallyl-aRNA Amplification Kit 1.0 (Epicentre Biotechnologies). The Bioanalyzer 2100 (Agilent Technologies) was used to determine the quality of the amplified RNA.

cDNA Library Preparation and Illumina RNA-Seq

The cDNA libraries were prepared using the standard Illumina mRNA-seq sample prep kits (revision D) and paired-end adaptors. The samples were run in single lanes on the Illumina Genome Analyzer model GAIIx. Transcript quantification of the RNA-seq data was performed using updated software as described previously (Li et al., 2010). Reads were aligned to the maize genome assembly (RefGen version 1; http://www.maizesequence.org) and the annotated exon junctions (version 4a53; http://www.maizesequence.org) with Burrows-Wheeler Alignment (Li and Durbin, 2009), allowing up to two mismatches. Reads assigned to each transcript were calculated by adding up reads aligned to exons and exon junctions.

Normalization and Identification of Differential Transcript Accumulation

Count data for each transcript were modeled as overdispersed Poisson random variables. The log of the Poisson mean for each count was modeled as the sum of a transcript-specific sample effect and an experimental unit–specific offset parameter. Following Bullard et al. (2010), the log of the upper quartile of the experimental unit–specific count distribution across transcripts was used as the offset to account for variation in library size across experimental units. A separate overdispersion parameter was estimated for each transcript using the sum of the squared Pearson residuals divided by the error degrees of freedom for each transcript ($12 - 6 = 6$). The small fraction of overdispersion parameter estimates that were less than 1 was replaced by 1 to disallow underdispersion.

For each transcript, tests for differences between sample effects were conducted by comparing the likelihood ratio statistic divided by the estimated overdispersion parameter to an F distribution with 6 denominator degrees of freedom and either 1 or 5 numerator degrees of freedom (1 for pairwise comparison of samples and 5 for the overall test for any differences among the six samples). The P values from these tests were converted to q values using the method of Nettleton et al. (2006). The q values were used to control FDRs as described previously (Storey and Tibshirani, 2003). Estimates of fold change between any pair of cell types were obtained by exponentiating the difference in sample effect estimates. Presence/absence of a transcript was determined using a threshold of 1 RPM.

Normalized expression level is reported as RPM, because laser microdissection and poly(A) tail–based RNA amplification methods result in a bias of sequence alignments toward the 3′ end of the transcript rather than equal distribution across the entire cDNA (Emrich et al., 2007; Li et al., 2010).

In Situ Hybridizations

Dissected seedlings and the remaining portions of the kernels or seedlings were fixed in formalin acetic acid alcohol, embedded, sectioned, and hybridized using gene-specific probes as previously described (Jackson, 1991). Gene-specific primers designed for probe synthesis can be found in Supplemental Table 1 online. Posthybridization slides were imaged using the Zeiss AxioCam MRc5 and AxioVision Release 4.6 software.

URLs

MapMan (http://gabi.rzpd.de/projects/MapMan/) was used to generate Supplemental Figures 2, 3, 5, 6, and 8 to 11 online.

Accession Numbers

RNA-seq data reported here have been deposited to MaizeGDB and are available online at http://www.maizegdb.org under Shoot Apical meristem at Six Stages (from Michael Scanlon's laboratory-SAM Group). Sequence data from this article can be found at MaizeGDB under the following accessions: GRMZM2G054795, *ZYB16*; GRMZM2G176390, *TDL1*; GRMZM2G094353, *RANBP2*; GRMZM2G040517, *OLE*; GRMZM2G101958,

*LTP*1*; GRMZM2G083725, *LTP*2*; GRMZM2G087267, *ALOG*1*; GRMZM2G038497, *UNK*1*; GRMZM073192, *UNK*2*; and GRMZM2G034385, *ALOG*2*.

Supplemental Data

The following materials are available in the online version of this article.

Supplemental Figure 1. Expression Pattern of *ZYB14* during Embryogenesis.

Supplemental Figure 2. Metabolic Overview of a Newly Formed Meristem Compared with a Mature Meristem Initiating Foliar Leaves.

Supplemental Figure 3. Regulatory Overview of a Newly Formed Meristem Compared with a Mature Meristem Initiating Foliar Leaves.

Supplemental Figure 4. Gene Clusters from Organ Initiation during Embryogenesis.

Supplemental Figure 5. Overview of Metabolic Gene Transcript Accumulation during Scutellum Elaboration Compared with during the Initiation of the First Foliar Leaf.

Supplemental Figure 6. Overview of Regulatory Gene Transcript Accumulation during Scutellum Elaboration Compared with during the Initiation of the First Foliar Leaf.

Supplemental Figure 7. Expression of *LTP*2* during Embryogenesis.

Supplemental Figure 8. Overview of Metabolic Gene Transcript Accumulation during Initiation of a Juvenile Leaf Compared with during Initiation of an Adult Leaf.

Supplemental Figure 9. Overview of Regulatory Gene Transcript Accumulation during Initiation of a Juvenile Leaf Compared with during Initiation of an Adult Leaf.

Supplemental Figure 10. Overview of Metabolic Gene Transcript Accumulation in the L14-Stage SAM Compared with in a Lateral Meristem.

Supplemental Figure 11. Overview of Metabolic Gene Transcript Accumulation in the L14-Stage SAM Compared with in a Lateral Meristem.

Supplemental Table 1. Gene List of Probes Used for in Situ Hybridizations.

Supplemental Table 2. Summary of RNA-Seq Reads and Alignments.

Supplemental Data Set 1. List of 226 Candidate Genes from the Heat Map Shown in Figure 2B.

Supplemental Data Set 2. Differentially Expressed Genes in the Proembryo Compared with all Meristem Samples.

Supplemental Data Set 3. Differentially Expressed Genes Present in Samples Containing a SAM.

Supplemental Data Set 4. Transcription Factors Upregulated in Samples Containing a SAM.

Supplemental Data Set 5. Differentially Expressed Genes in the Transition Stage Compared with the L14 Stage.

Supplemental Data Set 6. Differentially Expressed Transcription Factors in the Transition Stage Compared with the L14 Stage.

Supplemental Data Set 7. Differentially Expressed Genes during the Transition Stage, Coleoptilar Stage, and L1 Stage.

Supplemental Data Set 8. Differentially Expressed Transcription Factors during the Transition Stage, Coleoptilar Stage, and L1 Stage.

Supplemental Data Set 9. Differentially Expressed Genes during Initiation of Juvenile, Adult, and Husk Leaves.

Supplemental Data Set 10. List of Differentially Expressed Genes during Vegetative Phase Change.

Supplemental Data Set 11. Overview of Metabolic Gene Transcript Accumulation in a Newly Formed Meristem Compared with a Mature Meristem.

Supplemental Data Set 12. Overview of Regulatory Gene Transcript Accumulation in the Newly Formed Meristem Compared with a Mature Meristem.

Supplemental Data Set 13. Overview of Metabolic Gene Transcript Accumulation in the Transition Stage Compared with the L1-Stage Embryo.

Supplemental Data Set 14. Overview of Regulatory Gene Transcript Accumulation in the Transition Stage Compared with the L1-Stage Embryo.

Supplemental Data Set 15. Overview of Metabolic Gene Transcript Accumulation during Initiation of Adult Leaves Compared with Initiation of Juvenile Leaves.

Supplemental Data Set 16. Overview of Regulatory Gene Transcript Accumulation during Initiation of Adult Leaves Compared with Initiation of Juvenile Leaves.

Supplemental Data Set 17. Overview of Metabolic Gene Transcript Accumulation in the L14 SAM Compared with a Lateral Meristem.

Supplemental Data Set 18. Overview of Regulatory Gene Transcript Accumulation in the L14 SAM Compared with a Lateral Meristem.

ACKNOWLEDGMENTS

This study was supported by National Science Foundation grant IOS 0820610.

AUTHOR CONTRIBUTIONS

E.M.T. prepared samples, performed laser microdissection, isolated and amplified RNA, analyzed data, and performed all in situ hybridizations except for Figures 8F to 8H, which were provided by M.C.P.T. L.P. and Q.S. aligned RNA-seq data to the maize genome assembly and calculated read counts. J.L., C.D., and D.N. performed the normalization and identification of differential transcript accumulation. D.J.-B., J.Y., G.J.M, P.S.S., M.C.P.T., and M.J.S. obtained funding for this project. E.M.T. and M.J.S. wrote the article with contributions to the Methods from D.N. and Q.S. D.J.-B., J.Y., G.J.M., P.S.S., M.C.P.T., Q.S., and D.N. contributed to the design and execution of data analysis and extensively edited the article.

Received April 17, 2012; revised June 26, 2012; accepted August 6, 2012; published August 21, 2012.

REFERENCES

Abbe, E.C., and Stein, O.L. (1954). The growth of the shoot apex in maize: Embryogeny. Am. J. Bot. **41:** 285–293.

Abedon, B.G., Hatfield, R.D., and Tracy, W.F. (2006). Cell wall composition in juvenile and adult leaves of maize (*Zea mays* L.). J. Agric. Food Chem. **54:** 3896–3900.

Aida, M., Ishida, T., and Tasaka, M. (1999). Shoot apical meristem and cotyledon formation during *Arabidopsis* embryogenesis:

Interaction among the CUP-SHAPED COTYLEDON and SHOOT MERISTEMLESS genes. Development **126:** 1563–1570.

Bellaoui, M., Pidkowich, M.S., Samach, A., Kushalappa, K., Kohalmi, S.E., Modrusan, Z., Crosby, W.L., and Haughn, G.W. (2001). The *Arabidopsis* BELL1 and KNOX TALE homeodomain proteins interact through a domain conserved between plants and animals. Plant Cell **13:** 2455–2470.

Boyd, L. (1931). Evolution in the monocotyledonous seedling, a new interpretation of the grass embryo. Trans. Bot. Soc. Edinburgh **30:** 286–302.

Brady, S.M., Orlando, D.A., Lee, J.Y., Wang, J.Y., Koch, J., Dinneny, J.R., Mace, D., Ohler, U., and Benfey, P.N. (2007). A high-resolution root spatiotemporal map reveals dominant expression patterns. Science **318:** 801–806.

Breuninger, H., Rikirsch, E., Hermann, M., Ueda, M., and Laux, T. (2008). Differential expression of WOX genes mediates apical-basal axis formation in the *Arabidopsis* embryo. Dev. Cell **14:** 867–876.

Brooks, L., III et al. (2009). Microdissection of shoot meristem functional domains. PLoS Genet. **5:** e1000476.

Bullard, J.H., Purdom, E., Hansen, K.D., and Dudoit, S. (2010). Evaluation of statistical methods for normalization and differential expression in mRNA-Seq experiments. BMC Bioinformatics **11:** 94.

Byrne, M.E. (2009). A role for the ribosome in development. Trends Plant Sci. **14:** 512–519.

Chuck, G., Cigan, A.M., Saeteurn, K., and Hake, S. (2007). The heterochronic maize mutant Corngrass1 results from overexpression of a tandem microRNA. Nat. Genet. **39:** 544–549.

Clarke, J.H., Tack, D., Findlay, K., Van Montagu, M., and Van Lijsebettens, M. (1999). The SERRATE locus controls the formation of the early juvenile leaves and phase length in *Arabidopsis*. Plant J. **20:** 493–501.

Emrich, S.J., Barbazuk, W.B., Li, L., and Schnable, P.S. (2007). Gene discovery and annotation using LCM-454 transcriptome sequencing. Genome Res. **17:** 69–73.

Evans, M.M.S. (2007). The indeterminate gametophyte1 gene of maize encodes a LOB domain protein required for embryo Sac and leaf development. Plant Cell **19:** 46–62.

Evans, M.M.S., Passas, H.J., and Poethig, R.S. (1994). Heterochronic effects of glossy15 mutations on epidermal cell identity in maize. Development **120:** 1971–1981.

Fujita, K., Furuse, F., Sawada, O., and Bandara, D. (1994). Effect of defoliation and ear removal on dry matter production and inorganic element absorption in sweet corn. Soil Sci. Plant Nutr. **40:** 581–591.

Haecker, A., Gross-Hardt, R., Geiges, B., Sarkar, A., Breuninger, H., Herrmann, M., and Laux, T. (2004). Expression dynamics of WOX genes mark cell fate decisions during early embryonic patterning in *Arabidopsis thaliana*. Development **131:** 657–668.

Hay, A., and Tsiantis, M. (2010). KNOX genes: Versatile regulators of plant development and diversity. Development **137:** 3153–3165.

Hultquist, J.F., and Dorweiler, J.E. (2008). Feminized tassels of maize mop1 and ts1 mutants exhibit altered levels of miR156 and specific SBP-box genes. Planta **229:** 99–113.

Ichihashi, Y., Horiguchi, G., Gleissberg, S., and Tsukaya, H. (2010). The bHLH transcription factor SPATULA controls final leaf size in *Arabidopsis thaliana*. Plant Cell Physiol. **51:** 252–261.

Jackson, D. (1991). In situ hybridization in plants. In Molecular Plant Pathology: A Practical Approach, D.J. Bowles, S.J. Gurr, and M. McPherson, eds (Oxford, UK: Oxford University Press).

Jackson, D., Veit, B., and Hake, S. (1994). Expression of maize KNOTTED1 related homeobox genes in the shoot apical meristem predicts patterns of morphogenesis in the vegetative shoot. Development **120:** 405–413.

Jia, Y., Lisch, D.R., Ohtsu, K., Scanlon, M.J., Nettleton, D., and Schnable, P.S. (2009). Loss of RNA-dependent RNA polymerase 2 (RDR2) function causes widespread and unexpected changes in the expression of transposons, genes, and 24-nt small RNAs. PLoS Genet. **5:** e1000737.

Juarez, M.T., Twigg, R.W., and Timmermans, M.C.P. (2004). Specification of adaxial cell fate during maize leaf development. Development **131:** 4533–4544.

Kaplan, D. R. (1996). Early plant development: From seed to seedling to established plant. In Principles of Plant Morphology, Chapter 5 (Berkeley, CA: Copy Central, University of California, Berkeley).

Kiesselbach, T.A. (1949). The structure and reproduction of corn. Nebraska Agric. Exp. Stn. Res. Bull. **161: 1–96.**

Kim, J.H., Choi, D., and Kende, H. (2003). The AtGRF family of putative transcription factors is involved in leaf and cotyledon growth in *Arabidopsis*. Plant J. **36:** 94–104.

Langdale, J.A., Zelitch, I., Miller, E., and Nelson, T. (1988). Cell position and light influence C4 versus C3 patterns of photosynthetic gene expression in maize. EMBO J. **7:** 3643–3651.

Laubinger, S., Sachsenberg, T., Zeller, G., Busch, W., Lohmann, J.U., Rätsch, G., and Weigel, D. (2008). Dual roles of the nuclear cap-binding complex and SERRATE in pre-mRNA splicing and microRNA processing in *Arabidopsis thaliana*. Proc. Natl. Acad. Sci. USA **105:** 8795–8800.

Lauter, N., Kampani, A., Carlson, S., Goebel, M., and Moose, S.P. (2005). microRNA172 down-regulates glossy15 to promote vegetative phase change in maize. Proc. Natl. Acad. Sci. USA **102:** 9412–9417.

Levesque, M.P., Vernoux, T., Busch, W., Cui, H., Wang, J.Y., Blilou, I., Hassan, H., Nakajima, K., Matsumoto, N., Lohmann, J.U., Scheres, B., and Benfey, P.N. (2006). Whole-genome analysis of the SHORT-ROOT developmental pathway in *Arabidopsis*. PLoS Biol. **4:** e143.

Li, H., and Durbin, R. (2009). Fast and accurate short read alignment with Burrows-Wheeler transform. Bioinformatics **25:** 1754–1760.

Li, P., et al. (2010). The developmental dynamics of the maize leaf transcriptome. Nat. Genet. **42:** 1060–1067.

Lotan, T., Ohto, M., Yee, K.M., West, M.A., Lo, R., Kwong, R.W., Yamagishi, K., Fischer, R.L., Goldberg, R.B., and Harada, J.J. (1998). *Arabidopsis* LEAFY COTYLEDON1 is sufficient to induce embryo development in vegetative cells. Cell **93:** 1195–1205.

Moreno-Risueno, M.A., Van Norman, J.M., Moreno, A., Zhang, J., Ahnert, S.E., and Benfey, P.N. (2010). Oscillating gene expression determines competence for periodic *Arabidopsis* root branching. Science **329:** 1306–1311.

Mizukami, Y., and Fischer, R.L. (2000). Plant organ size control: AINTEGUMENTA regulates growth and cell numbers during organogenesis. Proc. Natl. Acad. Sci. USA **97:** 942–947.

Moose, S.P., and Sisco, P.H. (1994). Glossy15 controls the epidermal juvenile-to-adult phase transition in maize. Plant Cell **6:** 1343–1355.

Moose, S.P., and Sisco, P.H. (1996). Glossy15, an APETALA2-like gene from maize that regulates leaf epidermal cell identity. Genes Dev. **10:** 3018–3027.

Mu, J., Tan, H., Zheng, Q., Fu, F., Liang, Y., Zhang, J., Yang, X., Wang, T., Chong, K., Wang, X.J., and Zuo, J. (2008). LEAFY COTYLEDON1 is a key regulator of fatty acid biosynthesis in Arabidopsis. Plant Physiol. **148:** 1042–1054.

Mukherjee, K., Brocchieri, L., and Bürglin, T.R. (2009). A comprehensive classification and evolutionary analysis of plant homeobox genes. Mol. Biol. Evol. **26:** 2775–2794.

Müller, J., Wang, Y., Franzen, R., Santi, L., Salamini, F., and Rohde, W. (2001). In vitro interactions between barley TALE homeodomain

proteins suggest a role for protein-protein associations in the regulation of Knox gene function. Plant J. **27:** 13–23.

Nardmann, J., Ji, J., Werr, W., and Scanlon, M.J. (2004). The maize duplicate genes narrow sheath1 and narrow sheath2 encode a conserved homeobox gene function in a lateral domain of shoot apical meristems. Development **131:** 2827–2839.

Nardmann, J., and Werr, W. (2009). Patterning of the maize embryo and the perspective of evolutionary developmental biology. In Handbook of Maize: Its Biology, J. Bennetzen and S. Hake, eds (New York: Springer).

Nardmann, J., Zimmermann, R., Durantini, D., Kranz, E., and Werr, W. (2007). WOX gene phylogeny in Poaceae: A comparative approach addressing leaf and embryo development. Mol. Biol. Evol. **24:** 2474–2484.

Nelson, T., Tausta, S.L., Gandotra, N., and Liu, T. (2006). Laser microdissection of plant tissue: What you see is what you get. Annu. Rev. Plant Biol. **57:** 181–201.

Nettleton, D., Hwang, J.T.G., Caldo, R.A., and Wise, R.P. (2006). Estimating the number of true null hypotheses from a histogram of p-values. J. Agric. Biol. Environ. Stat. **11:** 337–356.

Nogueira, F.T.S., Chitwood, D.H., Madi, S., Ohtsu, K., Schnable, P.S., Scanlon, M.J., and Timmermans, M.C.P. (2009). Regulation of small RNA accumulation in the maize shoot apex. PLoS Genet. **5:** e1000320.

Oh, E., Yamaguchi, S., Hu, J., Yusuke, J., Jung, B., Paik, I., Lee, H. S., Sun, T.P., Kamiya, Y., and Choi, G. (2007). PIL5, a phytochrome-interacting bHLH protein, regulates gibberellin responsiveness by binding directly to the GAI and RGA promoters in *Arabidopsis* seeds. Plant Cell **19:** 1192–1208.

Ohtsu, K., et al. (2007). Global gene expression analysis of the shoot apical meristem of maize (*Zea mays* L.). Plant J. **52:** 391–404.

Pengelly, J.J., Kwasny, S., Bala, S., Evans, J.R., Voznesenskaya, E.V., Koteyeva, N.K., Edwards, G.E., Furbank, R.T., and von Caemmerer, S. (2011). Functional analysis of corn husk photosynthesis. Plant Physiol. **156:** 503–513.

Poethig, R.S., and Coe, E.H. Jr., and Johri, M.M. (1986). Cell lineage patterns in maize embryogenesis: A clonal analysis. Dev. Biol. **117:** 392–404.

Poethig, R.S. (1988). Heterochronic mutations affecting shoot development in maize. Genetics **119:** 959–973.

Poethig, R.S. (1990). Phase change and the regulation of shoot morphogenesis in plants. Science **250:** 923–930.

Randolph, L.F. (1936). Developmental morphology of the caryopsis in maize. J. Agric. Res. **53:** 881–916.

Reiser, L., Sánchez-Baracaldo, P., and Hake, S. (2000). Knots in the family tree: Evolutionary relationships and functions of knox homeobox genes. Plant Mol. Biol. **42:** 151–166.

Santa-Catarina, C., de Oliveira, R.R., Cutri, L., Floh, E.I.S., and Dornelas, M.C. (2012). WUSCHEL-related genes are expressed during somatic embryogenesis of the basal angiosperm *Ocotea catharinensis* Mez. (Lauraceae). Trees: Structure and Function **26: 493–501.**

Sarojam, R., Sappl, P.G., Goldshmidt, A., Efroni, I., Floyd, S.K., Eshed, Y., and Bowman, J.L. (2010). Differentiating *Arabidopsis* shoots from leaves by combined YABBY activities. Plant Cell **22:** 2113–2130.

Sawada, O., Ito, J., and Fujita, K. (1995). Characteristics of photosynthesis and translocation of 13C-labelled photosynthates in husk leaves of sweet corn. Crop Sci. **35:** 480–485.

Scanlon, M.J., Ohtsu, K., Timmermans, M.C.P. and Schnable, P.S. (July 1, 2009). Laser microdissection-mediated isolation and in vitro transcriptional amplification of plant RNA. Curr. Prot. Mol. Biol. **87** (online), doi/10.1002/0471142727.mb25a03s87.

Schnable, P.S., et al. (2009). The B73 maize genome: Complexity, diversity, and dynamics. Science **326:** 1112–1115.

Sen, T.Z., Andorf, C.M., Schaeffer, M.L., Harper, L.C., Sparks, M.E., Duvick, J., Brendel, V.P., Cannon, E., Campbell, D.A., and Lawrence, C.J. (2009). MaizeGDB becomes 'sequence-centric'. Database (Oxford) 2009, (online), doi/10.1093/database/bap020.

Shen, B., Allen, W.B., Zheng, P., Li, C., Glassman, K., Ranch, J., Nubel, D., and Tarczynski, M.C. (2010). Expression of ZmLEC1 and ZmWRI1 increases seed oil production in maize. Plant Physiol. **153:** 980–987.

Siegfried, K.R., Eshed, Y., Baum, S.F., Otsuga, D., Drews, G.N., and Bowman, J.L. (1999). Members of the YABBY gene family specify abaxial cell fate in *Arabidopsis*. Development **126:** 4117–4128.

Smith, H.M.S., Boschke, I., and Hake, S. (2002). Selective interaction of plant homeodomain proteins mediates high DNA-binding affinity. Proc. Natl. Acad. Sci. USA **99:** 9579–9584.

Smith, L.G., Greene, B., Veit, B., and Hake, S. (1992). A dominant mutation in the maize homeobox gene, Knotted-1, causes its ectopic expression in leaf cells with altered fates. Development **116:** 21–30.

Smith, L.G., Jackson, D., and Hake, S. (1995). Expression of knotted1 marks shoot meristem formation during maize embryogenesis. Dev. Genet. **16:** 344–348.

Storey, J.D., and Tibshirani, R. (2003). Statistical significance for genomewide studies. Proc. Natl. Acad. Sci. USA **100:** 9440–9445.

Strable, J., Borsuk, L., Nettleton, D., Schnable, P.S., and Irish, E.E. (2008). Microarray analysis of vegetative phase change in maize. Plant J. **56:** 1045–1057.

Suzuki, M., Latshaw, S., Sato, Y., Settles, A.M., Koch, K.E., Hannah, L.C., Kojima, M., Sakakibara, H., and McCarty, D.R. (2008). The Maize Viviparous8 locus, encoding a putative ALTERED MERISTEM PROGRAM1-like peptidase, regulates abscisic acid accumulation and coordinates embryo and endosperm development. Plant Physiol. **146:** 1193–1206.

Thimm, O., Bläsing, O., Gibon, Y., Nagel, A., Meyer, S., Krüger, P., Selbig, J., Müller, L.A., Rhee, S.Y., and Stitt, M. (2004). MAPMAN: A user-driven tool to display genomics data sets onto diagrams of metabolic pathways and other biological processes. Plant J. **37:** 914–939.

Tsuchiya, T., and Eulgem, T. (2010). Co-option of EDM2 to distinct regulatory modules in *Arabidopsis thaliana* development. BMC Plant Biol. **10: 203.**

Tzafrir, I., Pena-Muralla, R., Dickerman, A., Berg, M., Rogers, R., Hutchens, S., Sweeney, T.C., McElver, J., Aux, G., Patton, D., and Meinke, D. (2004). Identification of genes required for embryo development in Arabidopsis. Plant Physiol. **135:** 1206–1220.

Vollbrecht, E., Reiser, L., and Hake, S. (2000). Shoot meristem size is dependent on inbred background and presence of the maize homeobox gene, *knotted1*. Development **127:** 3161–3172.

Vroemen, C.W., Mordhorst, A.P., Albrecht, C., Kwaaitaal, M.A., and de Vries, S.C. (2003). The CUP-SHAPED COTYLEDON3 gene is required for boundary and shoot meristem formation in *Arabidopsis*. Plant Cell **15:** 1563–1577.

Weatherwax, P. (1920). Position of the scutellum and homology of coleoptile in maize. Bot. Gaz. **69:** 179–182.

Weijers, D., Franke-van Dijk, M., Vencken, R.J., Quint, A., Hooykaas, P., and Offringa, R. (2001). An *Arabidopsis* Minute-like phenotype caused by a semi-dominant mutation in a RIBOSOMAL PROTEIN S5 gene. Development **128:** 4289–4299.

Wu, X., Chory, J., and Weigel, D. (2007). Combinations of WOX activities regulate tissue proliferation during *Arabidopsis* embryonic development. Dev. Biol. **309:** 306–316.

Yamaguchi, T., Nagasawa, N., Kawasaki, S., Matsuoka, M., Nagato, Y., and Hirano, H.Y. (2004). The YABBY gene DROOPING LEAF regulates carpel specification and midrib development in *Oryza sativa*. Plant Cell **16:** 500–509.

Zhang, D.F., Li, B., Jia, G.Q., Zhang, T.F., Dai, J.R., Li, J.S., and Wang, S.C. (2008). Isolation and characterization of genes encoding GRF transcription factors and GIF transcriptional coactivators in maize (*Zea mays* L.). Plant Sci. **175:** 809–817.

Zhang, S., Wong, L., Meng, L., and Lemaux, P.G. (2002). Similarity of expression patterns of knotted1 and ZmLEC1 during somatic and zygotic embryogenesis in maize (*Zea mays* L.). Planta **215:** 191–194.

Zhang, X., Madi, S., Borsuk, L., Nettleton, D., Elshire, R.J., Buckner, B., Janick-Buckner, D., Beck, J., Timmermans, M., Schnable, P.S., and Scanlon, M.J. (2007). Laser microdissection of narrow sheath mutant maize uncovers novel gene expression in the shoot apical meristem. PLoS Genet. **3:** e101.

Zhao, Y., Medrano, L., Ohashi, K., Fletcher, J.C., Yu, H., Sakai, H., and Meyerowitz, E.M. (2004). HANABA TARANU is a GATA transcription factor that regulates shoot apical meristem and flower development in *Arabidopsis*. Plant Cell **16:** 2586–2600.

Zimmermann, R., and Werr, W. (2005). Pattern formation in the monocot embryo as revealed by NAM and CUC3 orthologues from *Zea mays* L. Plant Mol. Biol. **58:** 669–685.

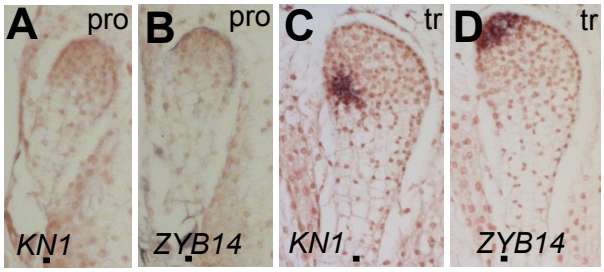

Supplemental Figure 1. Expression pattern of *ZYB14* during embryogenesis.

Side-by-side *in situ* hybridizations on consecutive sections using a *KN1* and a *ZYB14* anti-sense probe at (**A-B**) the proembryo or (**C-D**) transition phase. pro, proembryo; tr, transition phase. Scale bars represent 100 μm.

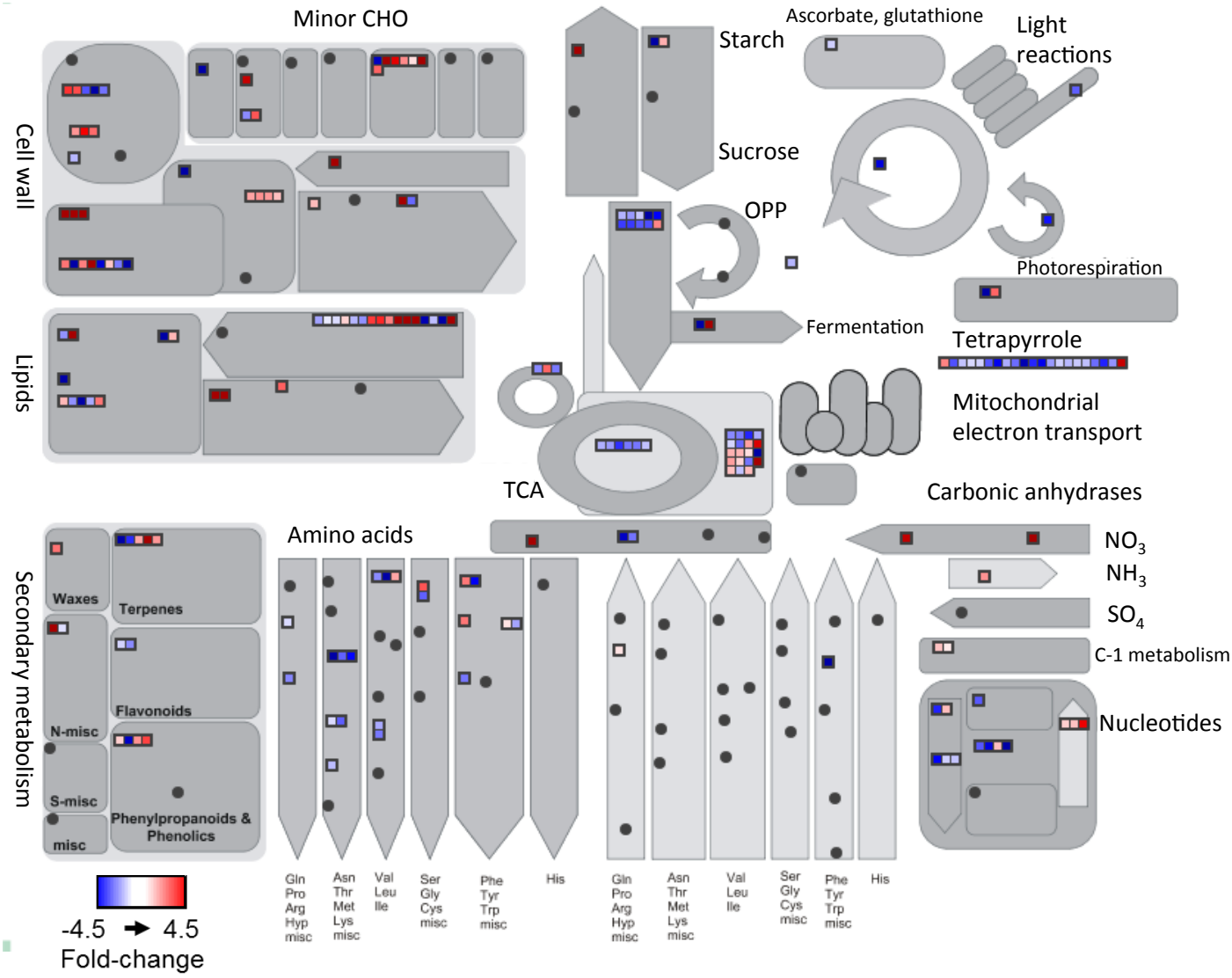

Supplemental Figure 2. Metabolic overview of a newly formed meristem compared to a mature meristem initiating foliar leaves.

Transcripts up-regulated in comparisons of a newly formed meristem and a mature meristem. In a newly formed meristem, transcripts implicated in amino acid synthesis, nucleotide metabolism, and mitochondrial electron transport/ATP synthesis are up-regulated. In a mature meristem, cell wall synthesis, minor CHO metabolism, nitrogen metabolism, and nucleotide degradation are up-regulated. Blue signifies that transcripts are up-regulated in a newly formed meristem, whereas red signifies that transcripts are up-regulated in a mature meristem. Squares represent differentially regulated transcripts present in each MapMan category. Closed circles indicate that there are no differentially regulated transcripts present in that MapMan category. The transcript list with detailed functional annotation is presented in Supplemental Dataset 6 online.

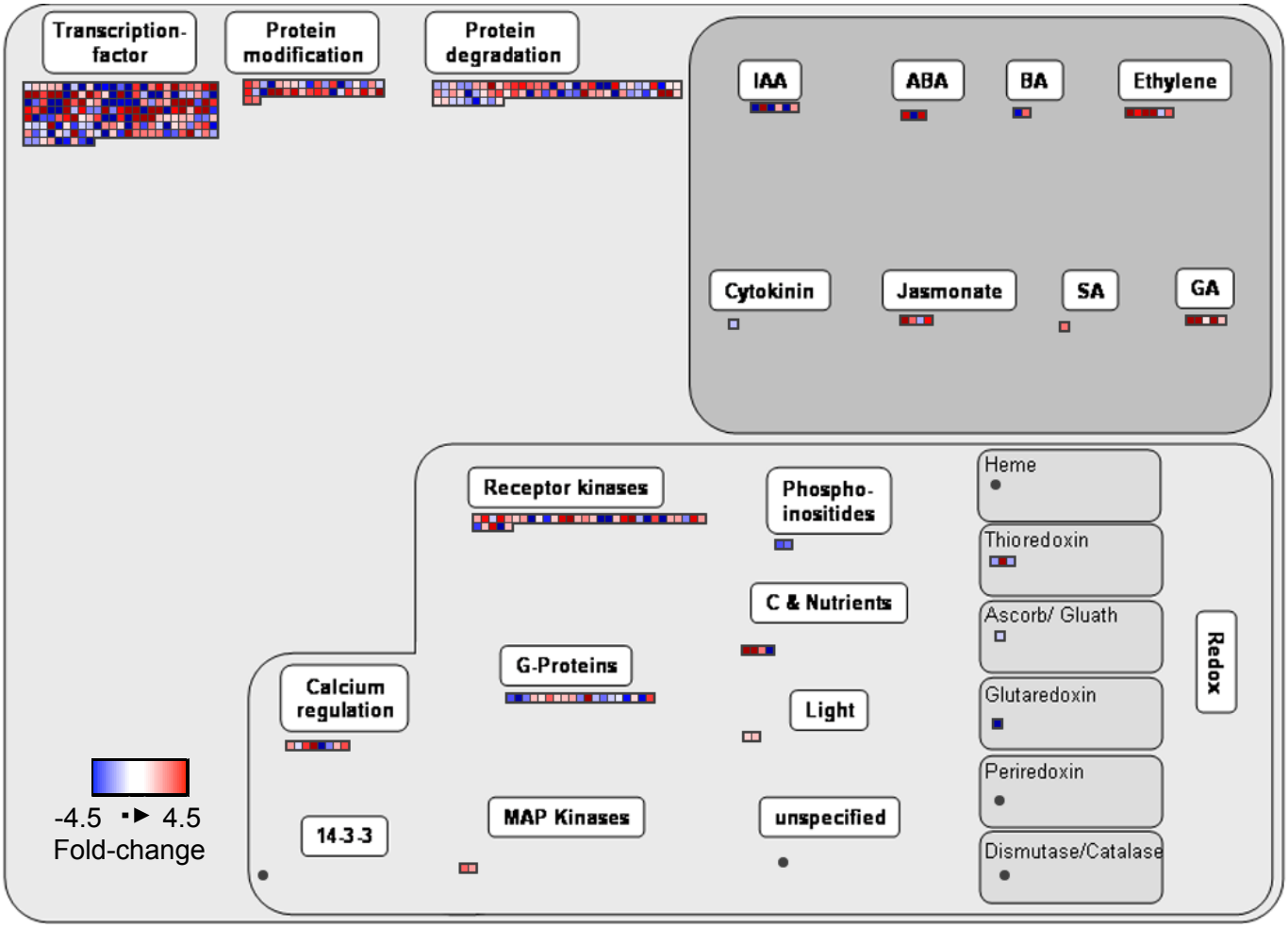

Supplemental Figure 3. Regulatory overview of a newly formed meristem compared to a mature meristem initiating foliar leaves.

Transcripts up-regulated in comparisons of a newly formed meristem and a mature meristem. In a mature meristem there are a greater number of up-regulated transcripts that function as transcription factors, in hormonal regulation, and in signaling. Blue signifies that transcripts are up-regulated in a newly formed meristem, whereas red signifies that transcripts are up-regulated in a mature meristem. Squares represent differentially regulated transcripts present in each MapMan category. Closed circles indicate that there are no differentially regulated transcripts present in that MapMan category. The transcript list with detailed functional annotation is presented in Supplemental Dataset 7 online.

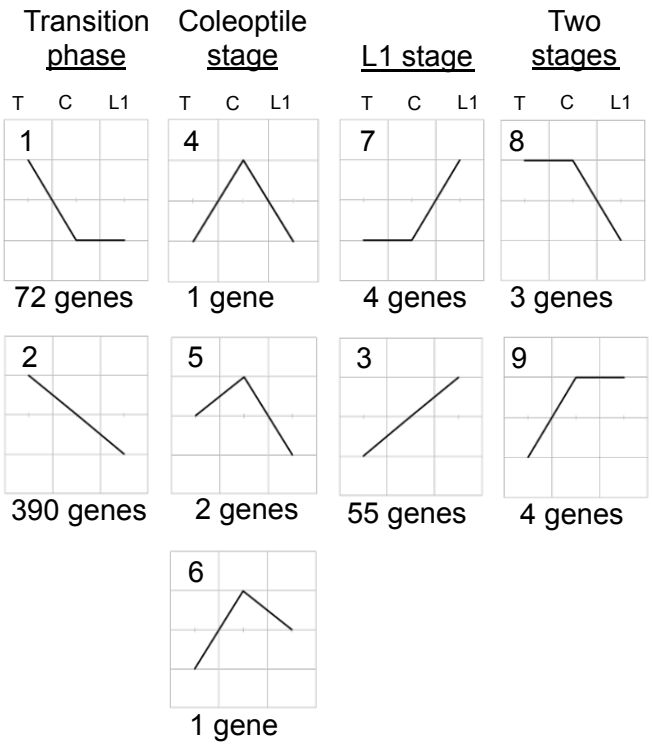

Supplemental Figure 4. Gene clusters from organ initiation during embryogenesis.

532 genes up-regulated from the three-way comparison of scutellum, coleoptile, and leaf initiation were sorted into nine clusters. Clusters include up-regulated in one stage over the two remaining stages (clusters 1, 4, and 7), up-regulated in one stage over one of the remaining stages (clusters 2, 5, 6, and 3), or in two stages over the remaining stage (clusters 8 and 9).

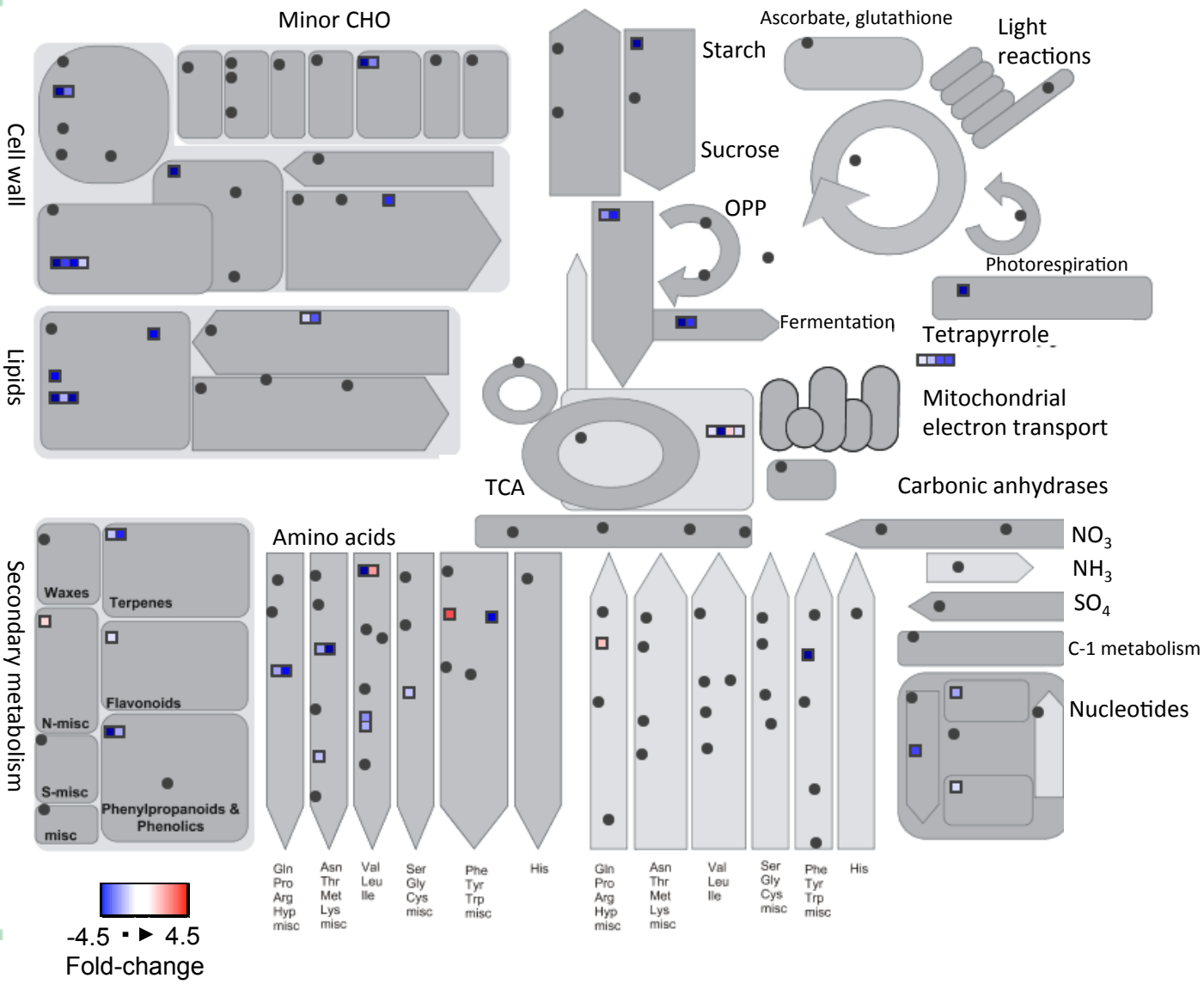

Supplemental Figure 5. Overview of metabolic gene transcript accumulation during scutellum elaboration compared to during the initiation of the first foliar leaf.

Transcripts up-regulated in comparisons of the elaboration of the scutellum and foliar leaf initiation. The majority of transcripts implicated in metabolism are up-regulated in the transition stage when the scutellum is being elaborated. Blue signifies that transcripts are up-regulated at the transition stage, whereas red signifies that transcripts are up-regulated at the L1 stage. Squares represent differentially regulated transcripts present in each MapMan category. Closed circles indicate that there are no differentially regulated transcripts present in that MapMan category. The transcript list with detailed functional annotation is included in Supplemental Dataset 10 online.

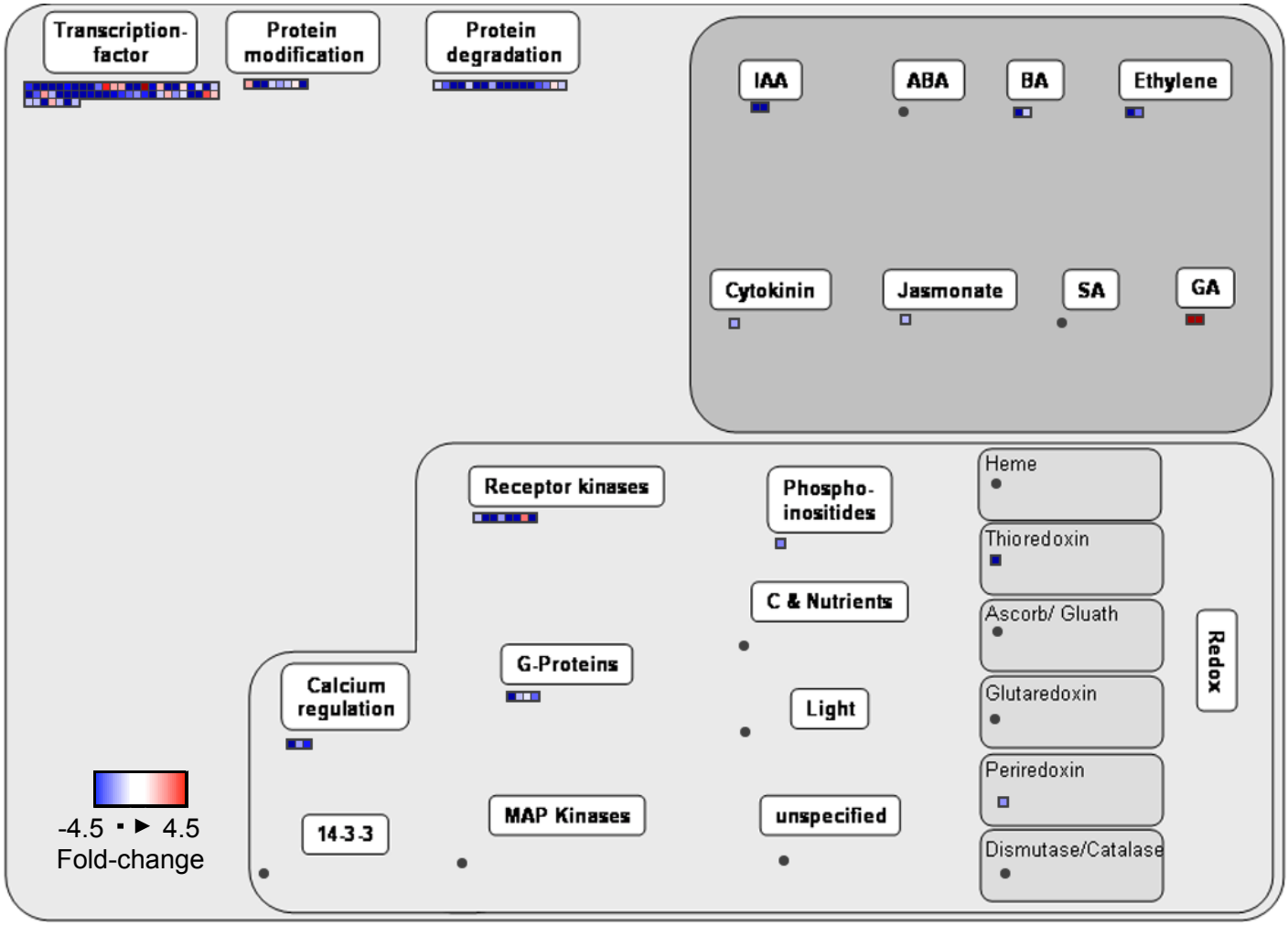

Supplemental Figure 6. Overview of regulatory gene transcript accumulation during scutellum elaboration compared to during the initiation of the first foliar leaf.

Transcripts up-regulated in comparisons of transition stage and L1 stage embryos. Most transcripts implicated in transcriptional regulation, hormone regulation, and signaling are up-regulated in the transition stage. However, two transcripts implicated in gibberellin synthesis and response are up-regulated when the first leaf is initiated at the L1 stage. Blue signifies that transcripts are up-regulated at the transition stage, whereas red signifies that transcripts are up-regulated at the L1 stage. Squares represent differentially regulated transcripts present in each MapMan category. Closed circles indicate that there are no differentially regulated transcripts present in that MapMan category. The transcript list with detailed functional annotation is presented in Supplemental Dataset 11 online.

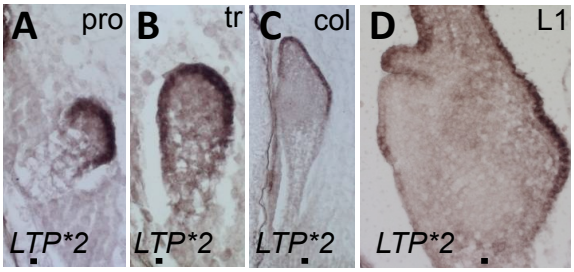

Supplemental Figure 7. Expression of *LTP*2* during embryogenesis.

In situ hybridization using *LTP*2* probe at (**A**) the proembryo, (**B**) transition phase, (**C**) coleoptile stage, and (**D**) the L1 stage. pro, proembryo; tr, transition phase; col, coleoptile stage; L1, leaf 1 stage. Scale bars represent 100 μm.

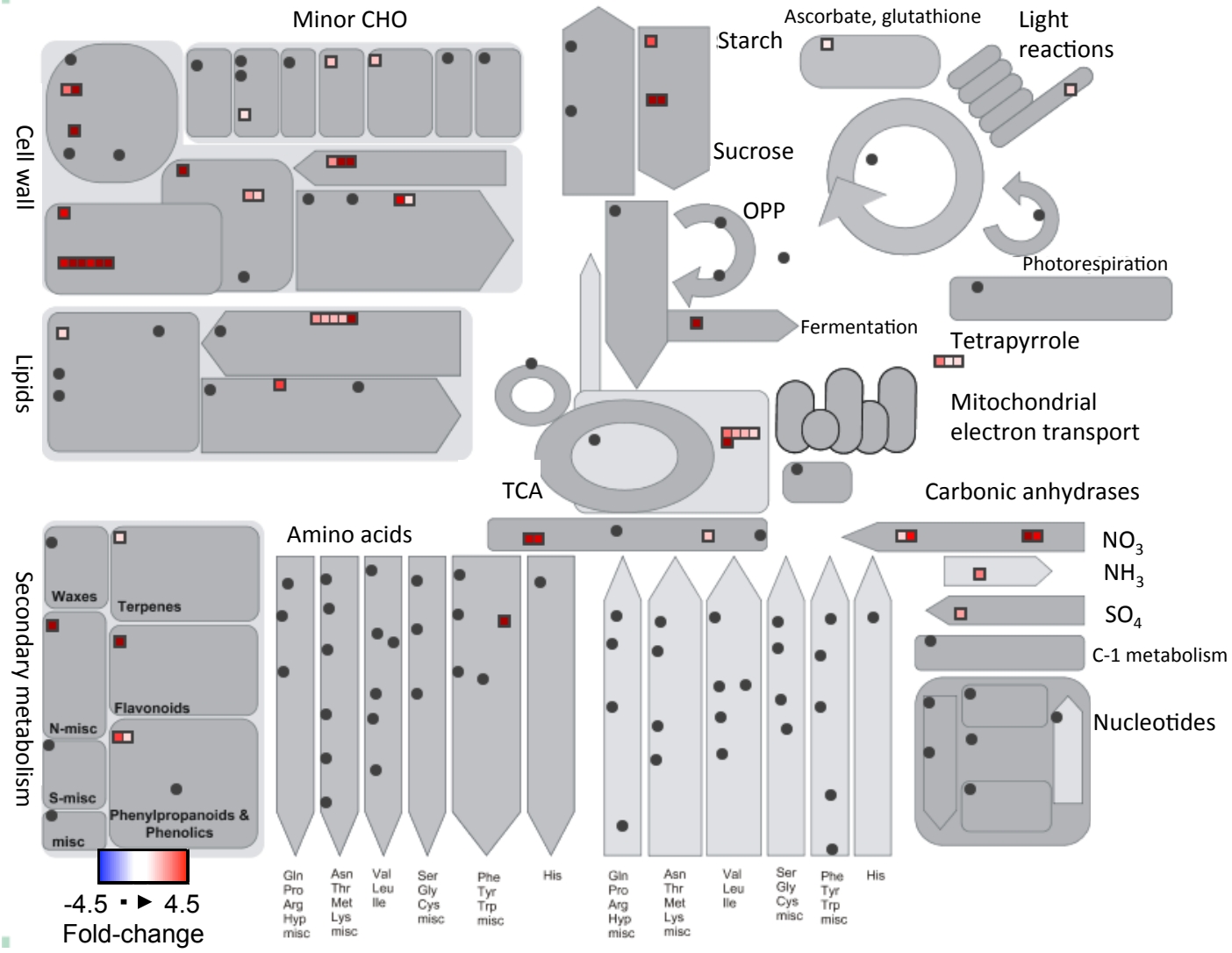

Supplemental Figure 8. Overview of metabolic gene transcript accumulation during initiation of a juvenile leaf compared to during initiation of an adult leaf.

Transcripts up-regulated in both husk leaves and L14 stage leaves compared to L1 stage leaves. Of the 57 up-regulated transcripts in adult leaves, the majority function in cell wall synthesis, lipid metabolism, secondary metabolism, and nitrogen metabolism. Fold-change is reported for the L14 stage leaf compared to the L1 stage leaf. Red signifies that transcripts are up-regulated at the L14 stage. Squares represent differentially regulated transcripts present in each MapMan category. Closed circles indicate that there are no differentially regulated transcripts present in that MapMan category. The transcript list with detailed functional annotation is presented in Supplemental Dataset 15 online.

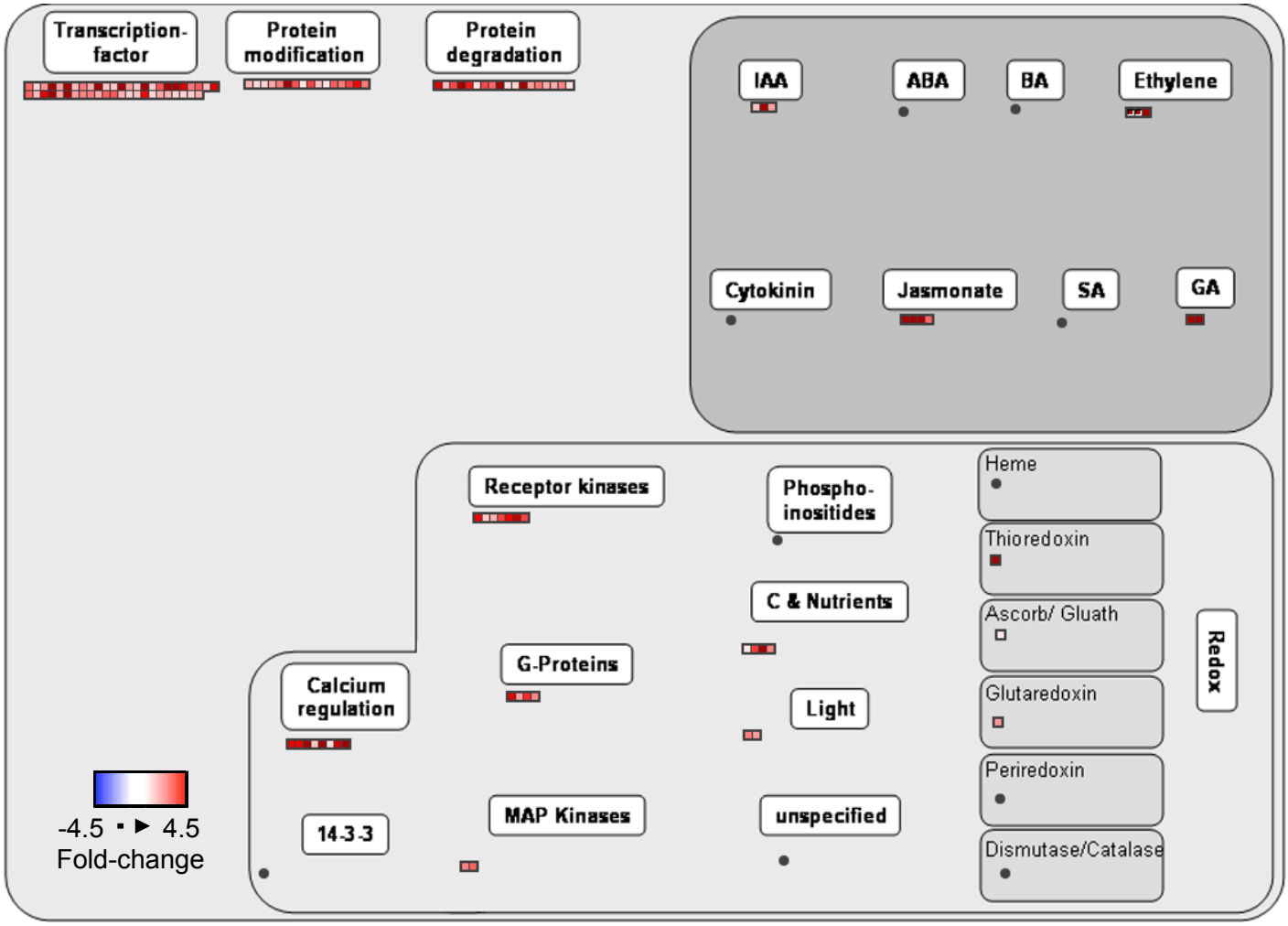

Supplemental Figure 9. Overview of regulatory gene transcript accumulation during initiation of a juvenile leaf compared to during initiation of an adult leaf.

The majority of the 124 up-regulated transcripts in adult leaves function in transcriptional regulation, protein modifications, protein degradation, and calcium signaling. Fold-change of the transcripts is reported for the L14 stage leaf compared to the L1 stage leaf. Red signifies that transcripts are up-regulated at the L14 stage. Squares represent differentially regulated transcripts present in each MapMan category. Closed circles indicate that there are no differentially regulated transcripts present in that MapMan category. The transcript list with detailed functional annotation is presented in Supplemental Dataset 16 online.

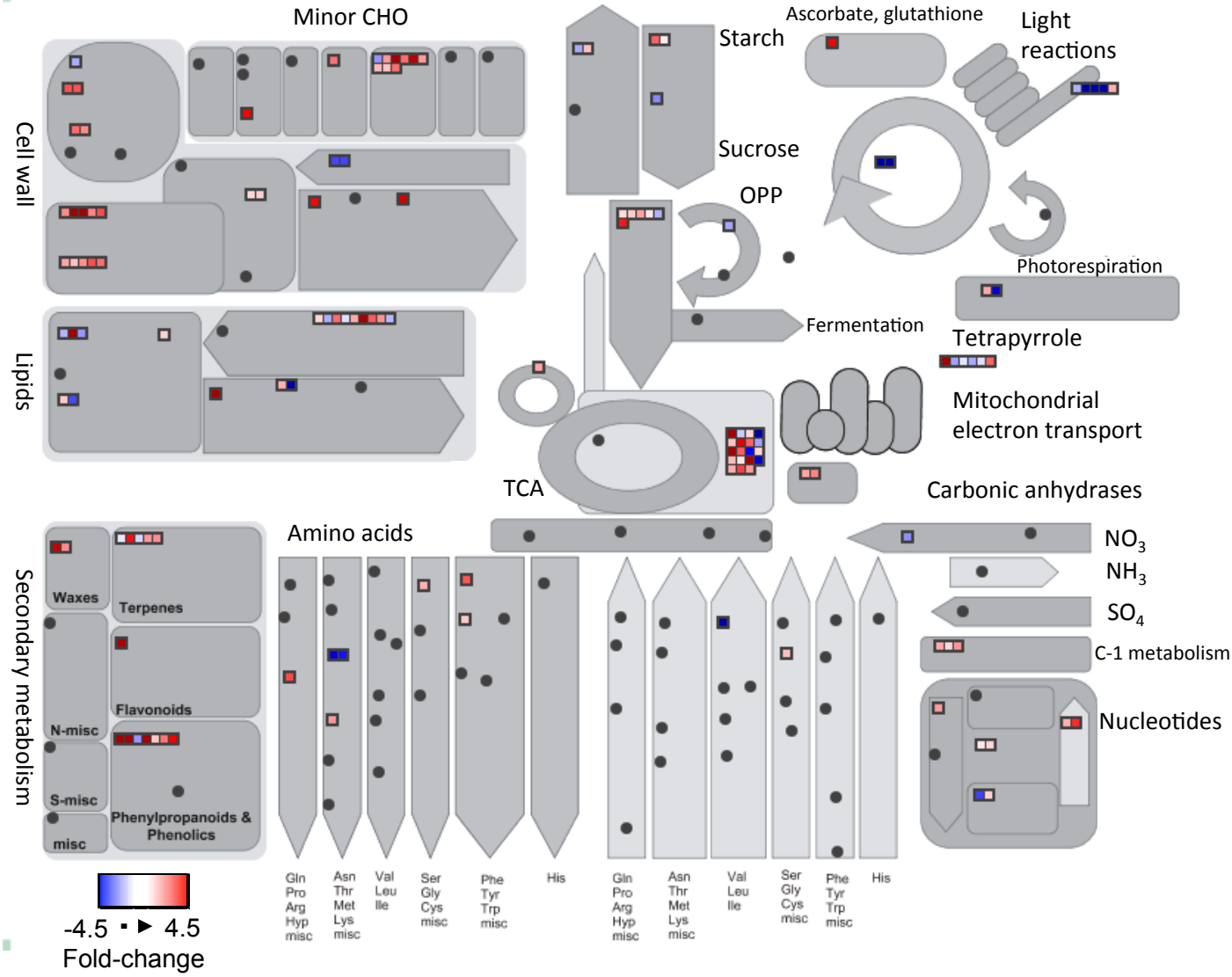

Supplemental Figure 10. Overview of metabolic gene transcript accumulation in the L14 stage SAM compared to in a lateral meristem.

Transcripts up-regulated in comparisons of a L14 SAM to a lateral meristem. Transcripts up-regulated in the L14 SAM function in cell wall synthesis, secondary metabolism, amino acid synthesis, and C1-metabolism. In lateral meristems, transcripts that function in light reactions, mitochondrial electron transport/ATP synthesis, and cell wall precursors are up-regulated. Blue signifies that transcripts are up-regulated in the lateral meristem, whereas red signifies that transcripts are up-regulated in the L14 SAM. Squares represent differentially regulated transcripts present in each MapMan category. Closed circles indicate that there are no differentially regulated transcripts present in that MapMan category. The transcript list with detailed functional annotation is presented in Supplemental Dataset 17 online.

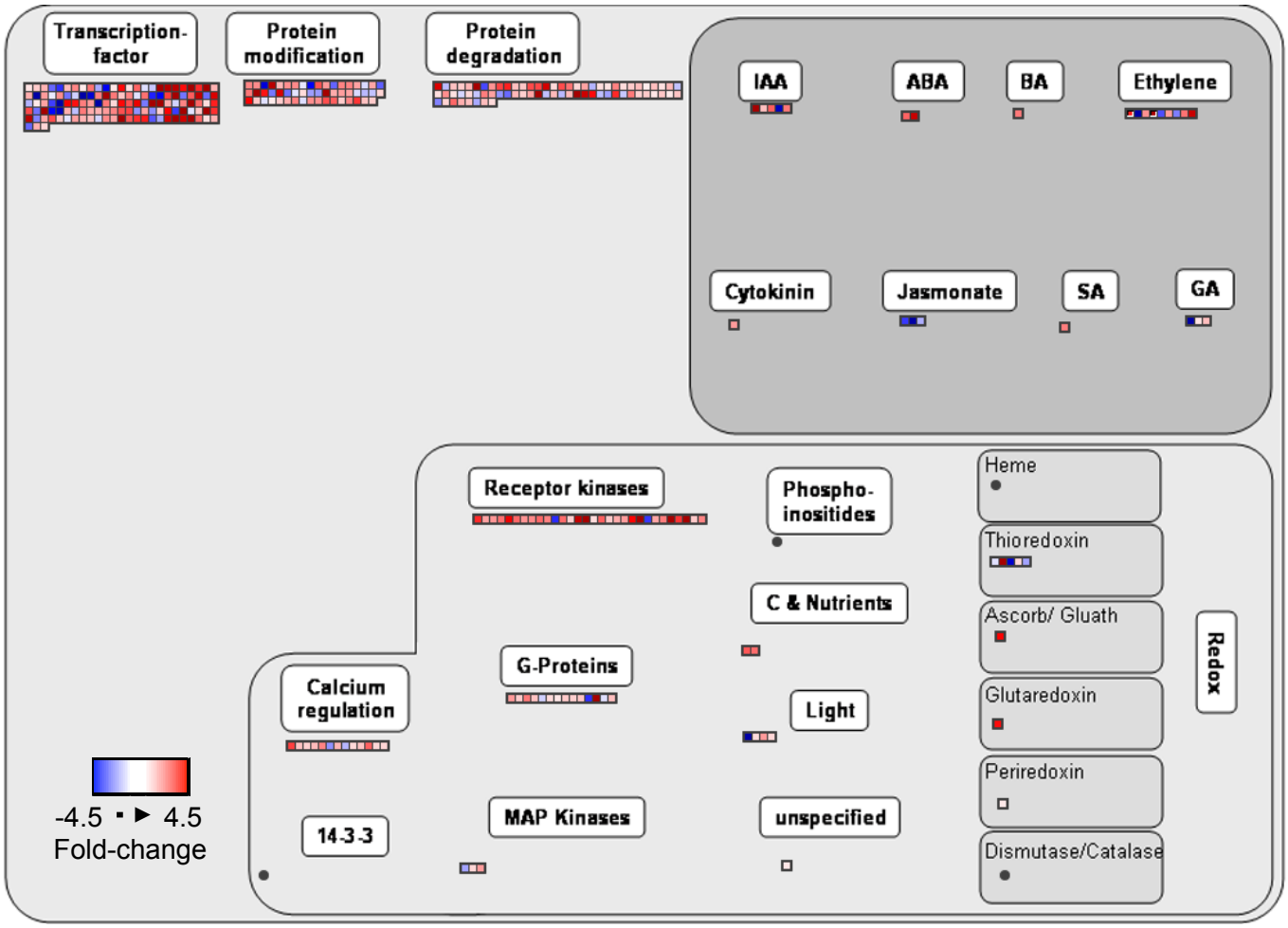

Supplemental Figure 11. Overview of metabolic gene transcript accumulation in the L14 stage SAM compared to in a lateral meristem.

Transcripts up-regulated in comparisons of L14 SAM to lateral meristem. Most transcripts that function in transcriptional regulation, protein modifications, protein degradation, hormonal regulation, and signaling are up-regulated in the L14 SAM. Blue signifies transcripts that are up-regulated in the lateral meristem, whereas red signifies that transcripts are up-regulated in the L14 SAM. Squares represent differentially regulated transcripts present in each MapMan category. Closed circles indicate that there are no differentially regulated transcripts present in that MapMan category. The transcript list with detailed functional annotation is presented in Supplemental Dataset 18 online.

Suppemental Table 1. Gene list of probes used for *in situ* hybridizations.

Gene name	Accession	Forward primer	Reverse primer	Product length (bp)	Expression (RPM) Proembryo	Transition phase	Coleoptile Stage	L1 stage	L14 stage	Lateral meristem
KNOTTED1	GRMZM2G017087	ACAAGGTGGGGGCACCA	TCGGTCTCTCCTCCGCTA	316	0.00	298.44	229.89	160.80	1599.88	245.50
Zea mays YABBY16	GRMZM2G054795	CTCATCCAATAACTCCAACAAAG	GATTTTGCATAGGGTTCTTCTTC	790	59.49	102.17	36.66	65.97	64.01	86.52
Zea mays YABBY14	GRMZM2G005353	CGACCTCACCGCACGGTCT	GAGCTCCCTCCTGAGTTTGC	447	0.00	60.85	59.62	82.24	8.60	67.96
ZEA MAYS LEAFY COTYLEDON1	GRMZM2G011789	GGACTCCAGCAGCTTCCT	GTACGCGTAAGGCAGGTAGT	658	216.85	502.98	93.70	0.01	0.00	0.00
TAPETUM DETERMINANT1-LIKE	GRMZM2G176390	GACAATGGTGCTTTAAGAAACG	GAGTTGGAGTACTGGAAGGAGAC	463	0.00	88.96	0.00	0.21	0.00	0.00
RAN BINDING PROTEIN2	GRMZM2G094353	GAACAGGAAGCCAGGAGACT	CAGTGCAAGTAGTTTTCGTAGGT	498	0.00	97.34	108.96	1.73	1.48	0.07
POLLEN OLE E I	GRMZM2G040517	CCTTGAAGGACCACTGTGC	GTACATGAGCGCAGTCTTGG	560	22.21	1018.19	83.34	6.98	1.04	2.42
LIPID TRANSFER PROTEIN1	GRMZM2G101958	CAGCTAGCTCTAGCAAAGCA	TTGCAAACAAAAAGAGGTGA	822	1578.26	4438.79	621.05	177.69	36.32	108.83
LIPID TRANSFER PROTEIN2	GRMZM2G083725	GCAGCCAAGCAAATAAAAGT	ACAAGTCACCATGAAACACG	847	144.11	210.66	36.87	43.10	43.66	82.12
ARABIDOPSIS LSH1 AND ORYZA G11	GRMZM2G087267	TCTCCTCAACCCACCATATT	GTGCGGGATCAAGAAGTG	791	2.32	15.08	33.81	134.91	69.84	116.82
UNKNOWN1	GRMZM2G038497	CTGTACCTGCAGAACTGCTACAT	CCCATCAACTAAAACTAGACAAACA	418	0.00	27.90	45.11	41.88	46.31	22.87
UNKNOWN2	GRMZM2G073192	GCTGCAGCTTTACCGATTCC	CTTACAAGCTCACCATCCAAAG	421	0.272895	27.66141	50.91464	36.050315	8.490335	18.493265
ARABIDOPSIS LSH1 AND ORYZA G12	GRMZM2G034385	GGTACGAGTCGCAGAAGC	ATCTGGTGCTCGTAGTGGTG	470	0.00	11.12	15.61	26.43	84.22	103.57
LIPID TRANSFER PROTEIN3	GRMZM2G093997*	CAACTCTTTCTCTCCTGCAA	CTACGTACTTGGTGCAGTCG	410	2.78	11.74	59.82	72.69	716.28	1666.84

*new accession: GRMZM5G898755

Supplemental Table 1. Gene list of probes used for *in situ* hybridizations.

Suppemental Table 2. Summary of RNAseq reads and alignments.

Sample	Number of replicates captured	Total area of tissue captured (μm2)	Total # of sequences (million)	Percent of unambiguous sequence alignments to maize gene space
Proembryo 1	7	221,338	17.7	41%
Proembryo 2	7	255,205	13	51%
Transition phase 1	3	695,787	10.6	62%
Transition phase 2	3	1,036,719	12.7	88%
Coleoptile stage 1	6	810,869	20.7	67%
Coleoptile stage 2	4	432,794	21.6	66%
L1 stage 1	6	343,410	18.3	71%
L1 stage 2	3	148,276	21.5	62%
L14 stage 1	5	1,279,864	14.2	77%
L14 stage 2	6	1,652,455	18.5	78%
Lateral meristems 1	6	503,008	16.7	52%
Lateral meristems 2	8	909,404	18.2	57%

Supplemental Table 2. Summary of RNAseq reads and alignments.